HDL-TR-1765

(1) FC.

A Direct Tunneling Model of Charge Transfer at the Insulator-Semiconductor Interface in MIS Devices

October 1976

SPONSORED IN PART BY THE DEFENSE NUCLEAR AGENCY UNDER DNA TASK Z99QAXTA008, WORK UNIT 51, WORK UNIT TITLE "PHYSICS OF TRE IN DIELECTRIC MATERIALS."

U.S. Army Materiel Development and Readiness Command
HARRY DIAMOND LABORATORIES
Adelphi, Maryland 20783

The findings in this report are not to be construed as an official Department of the Army position unless so designated by other authorized documents.

Citation of manufacturers' or trade names does not constitute an official indorsement or approval of the use thereof.

Destroy this report when it is no longer needed. Do not return it to the originator.

UNCLASSIFIED

SECURITY CLASSIFICATION OF THIS PAGE (When Data Entered)

REPORT DOCUMENTATION PAGE	READ INSTRUCTIONS BEFORE COMPLETING FORM
1. REPORT NUMBER: HDL-TR-1765	2. GOVT ACCESSION NO. — 3. RECIPIENT'S CATALOG NUMBER
4. TITLE (and Subtitle): A Direct Tunneling Model of Charge Transfer at the Insulator-Semiconductor Interface in MIS Devices.	5. TYPE OF REPORT & PERIOD COVERED: Technical Report, 6. PERFORMING ORG. REPORT NUMBER
7. AUTHOR(s): Flynn B. McLean	8. CONTRACT OR GRANT NUMBER(s): DA: 1T161102B11A
9. PERFORMING ORGANIZATION NAME AND ADDRESS: Harry Diamond Laboratories, 2800 Powder Mill Road, Adelphi, MD 20783	10. PROGRAM ELEMENT, PROJECT, TASK AREA & WORK UNIT NUMBERS: Program Element: 6.11.02.B, 6.27.04.H
11. CONTROLLING OFFICE NAME AND ADDRESS: Defense Nuclear Agency, Washington, DC 20305	12. REPORT DATE: Oct 76; 13. NUMBER OF PAGES: 47 (42 p.)
14. MONITORING AGENCY NAME & ADDRESS (if different from Controlling Office)	15. SECURITY CLASS. (of this report): Unclassified; 15a. DECLASSIFICATION/DOWNGRADING SCHEDULE

16. DISTRIBUTION STATEMENT (of this Report)

Approved for public release; distribution unlimited.

17. DISTRIBUTION STATEMENT (of the abstract entered in Block 20, if different from Report)

18. SUPPLEMENTARY NOTES

HDL Projects: A11537 & 335535 DRCMS Codes: 611102.11.85100, 697000.22.11264

Sponsored in part by the Defense Nuclear Agency under DNA Task Z99QAXTA008, Work Unit 51, Work Unit Title "Physics of TRE in Dielectric Materials."

19. KEY WORDS (Continue on reverse side if necessary and identify by block number)

MIS devices
Charge injection
Radiation effects
Insulator-semiconductor interface effects
Electron tunneling theory

20. ABSTRACT (Continue on reverse side if necessary and identify by block number)

A general model of charge transfer at the insulator-semiconductor interface of metal-insulator-semiconductor (MIS) devices is developed. The model is based upon direct WKB tunneling of electrons from the semiconductor substrate into localized trap states within the forbidden gap of the insulator. Both an arbitrary distribution of the insulator states in energy as well as spatial variation in the trap densities in the interface region

over

DD FORM 1 JAN 73 1473 EDITION OF 1 NOV 65 IS OBSOLETE 1 UNCLASSIFIED

SECURITY CLASSIFICATION OF THIS PAGE (When Data Entered)

163 050

are treated. Advantage is taken of the strong spatial decay of the tunneling transition probability to obtain valid approximate solutions of the tunneling equations in a form directly amenable to numerical evaluation. The effects of internal electric fields in the insulator are included in a self-consistent manner. The results of several representative model calculations of post-irradiation annealing and field-injection characteristics of MIS capacitors are described.

CONTENTS

FIGURES

FIGURES (Cont'd)

1. INTRODUCTION

A model is developed of the charge transfer processes occurring at the insulator-semiconductor interface of the gate insulator in metal-insulator-semiconductor (MIS) devices. This model is based upon direct WKB tunneling of electrons into localized trap states in the insulator. The model is directed toward a general description of both annealing of holes that have been trapped in an interface region after exposure to ionizing radiation as well as the bias instability (field-induced charge injection) observed in Al_2O_3 MIS devices. The mathematical framework of the model is described and representative model calculations of postirradiation annealing and field-injection characteristics of MIS capacitors are presented. A detailed analysis of rapid annealing and charge injection data on Al_2O_3 MIS capacitors in terms of the tunneling model has been described elsewhere.[1]

Two of the essential features* that must be explained by a successful theory of charge transfer are (1) the strong bias dependence of the field-injection characteristics in the Al_2O_3 devices, and (2) the prevailing logarithmic dependence of the transferred charge on time. The logarithmic time dependence is true both in the charging by field injection in Al_2O_3 devices and in annealing of positive charge after irradiation in both Al_2O_3 and SiO_2 MIS devices.[1,*] The direct tunneling model does predict these general features, and it also allows quantitative information concerning the oxide trap distributions near the interface to be extracted from the analysis of experimental data. We should point out that the short-term annealing characteristics of SiO_2 MIS capacitors

---

*See Annotated Bibliography, Charge Injection and Post-Irradiation Rapid Annealing in MOS Devices.

[1] F. B. McLean, H. E. Boesch, Jr., P. S. Winokur, J. M. McGarrity, and R. B. Oswald, Jr., IEEE Trans. Nucl. Sci. NS-21 (1974), 47.

have recently been shown[2,3] to be dominated by a stochastic hopping transport of holes to the interface, but there remains a long-term logarithmic annealing of the positive charge that occurs after most of the holes have transported to or through the interface. This long-term annealing process may be attributed[4] to relaxation of a trapped-hole distribution in the interface region via tunneling of electrons from the Si substrate with subsequent recombination with the trapped holes.

The modeling of the charge transfer at the gate insulator interfaces employs single electron WKB theory[5] for electrons tunneling directly from the electronic energy bands of the substrate material (normally Si) or gate metal into localized electron states with energies in the forbidden gap of the insulator. It draws to some extent upon the idea behind a certain class of metal-nitride-oxide-semiconductor (MNOS) memory transistors.* The physical basis of the model is also similar to that underlying the theory of the frequency response of surface states in MIS systems.† The theory is developed formally in a general way and includes in principle both energy conserving and energy nonconserving processes (e.g., phonon-assisted tunneling) as well as three-dimensional effects. The localized insulator states are either electron traps, as for field injection, or occupied hole traps in postirradiation annealing. The model treats both an arbitrary energy distribution of

---

*See Annotated Bibliography, Theory of MNOS Memory Transistors.

†See Annotated Bibliography, Theory of Frequency Reponse of Surface States.

[2] F. B. McLean, G. A. Ausman, Jr., H. E. Boesch, Jr., and J. M. McGarrity, J. Appl. Phys. 49 (1976), 1529.

[3] H. E. Boesch, Jr., F. B. McLean, J. M. McGarrity, and G. A. Ausman, Jr., IEEE Trans. Nucl. Sci. NS-22 (1975), 2163.

[4] R. J. Maier, Summaries of Papers, IEEE Annual Conf. on Nucl. and Space Radiation Effects, Seattle (1972), 215.

[5] C. B. Duke, Tunneling in Solids, Academic Press, New York (1969), p. 30.

insulator states as well as spatial variation in the trap densities in the interface regions. The known energy-band structure of silicon (or the gate metals) convoluted with the capture cross sections of the insulator states is used as the "supply function" for the tunneling electrons. The effects of internal electric fields in the insulator are included in a self-consistent fashion by solving Poisson's equation along with the tunneling equations (i.e., the change in the internal electric fields due to the accumulation of tunneling charge is accounted for).

In section 2 the general theory is formulated and illustrated by the exact solution for a simple case, namely, that of a single trap level with uniform spatial distribution. In section 3 the general theory is developed analytically to the point where the solutions can be obtained numerically by simple quadrature. This is accomplished by means of a set of simplifying approximations which are justified on physical grounds. In section 4 details of the numerical procedure are described, and model calculations for several representative cases important in practice are presented. First, the field-injection characteristics for Al_2O_3 devices are described for two cases: (1) where a thin SiO_2 layer is present between the Si substrate and the deposited Al_2O_3, and (2) where no SiO_2 layer is present. The important qualitative features distinguishing these two cases are pointed out. Second, the charge relaxation characteristics following irradiation due to tunneling/recombination of a trapped-hole distribution in the interface region is discussed. Particular emphasis is placed upon the effects produced by spatial variation of the trapped-hole distribution. In the last section the main results are summarized, and a brief discussion is given of the application of the model to the analysis of experimental data.

2. FORMAL THEORY

Let $N(E,x)$ be the arbitrary distribution of insulator traps, both in energy E and distance x from the tunneling interface (insulator-semiconductor interface). Energy values will be referenced to the valence band edge of the insulator (fig. 1). Let $n(E,x,t)$ be the distribution of traps occupied at time t. We assume that at time $t = 0$ all traps are unoccupied, i.e., $n(E,x,0) = 0$. Next, we define a function $g(E,x,t)$ that gives the probability per unit time that an electron will make a tunneling transition from the substrate material to a single unoccupied trap of energy E located at the distance x at time t. The function $g(E,x,t)$ is essentially a Green's function for the tunneling transition rate; it is time dependent when the internal electric field in the interface region is time dependent, as is the case when the charge distributions are changing significantly due to the charge transfer process. The tunneling transition rate $T(E,x,t)$ to traps of energy E at distance x from the interface is simply the product of $g(E,x,t)$ and the unoccupied trap density

$$T(E,x,t) = g(E,x,t)\,[N(E,x) - n(E,x,t)] \tag{1}$$

But this is also equal to the time rate of change of the occupied trap distribution

$$\frac{dn}{dt}(E,x,t) = T(E,x,t) \tag{2}$$

the solution of which is

$$n(E,x,t) = N(E,x)\left\{1 - \exp\left[-\int_0^t dt' g(E,x,t')\right]\right\} \tag{3}$$

The total tunneling current per unit area $J(t)$ is then given by the double integral of $T(E,x,t)$ over all E and x. Using equation (3), we have the formal solution for the tunneling current

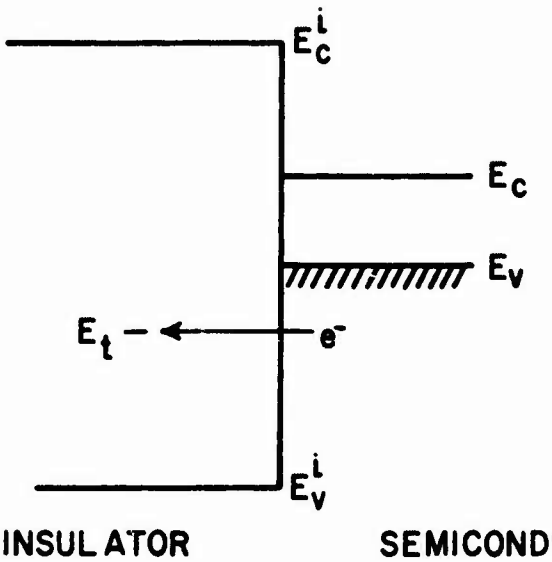

Figure 1. Schematic band diagram of the insulator-semiconductor interface in an MIS system at zero bias. Distance is measured with respect to the interface and energies are measured relative to E_v^i, the valence band edge of the insulator. E_t represents a localized trap state in the insulator, which acts as a recipient for electrons tunneling from the semiconductor substrate.

$$J(t) = e\int_o^\infty dx \int_o^{E_c^i} dE g(E,x,t) N(E,x) \exp\left[-\int_o^t dt' g(E,x,t')\right] \qquad (4)$$

where e is the electronic charge and E_c^i is the conduction band edge of the insulator (measured relative to the insulator valence band edge). The total charge transferred at time t is simply

$$Q(t) = \int_o^t dt' J(t') \qquad (5)$$

It should be noted that J(t) is not the current that would be measured by an external circuit, but is the charge flux at the tunneling interface. The externally measured current would be much smaller, due to the small displacement of the tunneling charge relative to the thickness of the insulator film.

The tunneling equations must be solved self-consistently with Poisson's equation to account for the relaxation of the energy bands due to the tunneled charge. This band relaxation is described by the time dependence of the electrostatic potential $\phi(x,t)$ given by

$$\phi(x,t) = \phi_i(x) - e\int_o^x \mathcal{E}(x',t)dx' \tag{6}$$

where ϕ_i is the image potential (important only very near the interface) and $\mathcal{E}(x,t)$ is the x component of the electric field. $\mathcal{E}(x,t)$ is found by the solution to Poisson's equation

$$\mathcal{E}(x,t) = \mathcal{E}_o(t) + \int_o^x dx' \frac{\rho(x',t)}{\varepsilon_i} \tag{7}$$

where $\mathcal{E}_o(t)$ is the field at $x = 0$, ε_i is the dielectric constant of the insulator, and $\rho(x,t)$ is the charge distribution in the insulator given by

$$\rho(x,t) = \rho_o(x) + e\int_o^{E_c^i} dE\, n(E,x,t) \tag{8}$$

where $\rho_o(x)$ is the initial charge distribution.

Equations (4) and (5) solved self-consistently with Poisson's equation thus constitute the formal solution to the tunneling problem. In essence the problem is reduced to determining the Green's function $g(E,x,t)$. Various approaches are possible to determine $g(E,x,t)$ with varying degrees of sophistication, such as whether one considers one- or three-dimensional tunneling, elastic (energy conserving) or inelastic tunneling. However, the only viable starting point for any approach is the one-electron WKB approximation. The essential results of this approximation are that we consider only one-electron transitions from the Bloch band states of the substrate solid to the localized insulator states and that the probability of making a

transition to a state at distance x from the interface is proportional tc the exponential factor exp(-Z(E,x,t)) where Z is essentially a scaled distance given by

$$Z(E,x,t) = 2\int_{o}^{x} dx' \, \beta(E,x't) \tag{9}$$

$$\beta(E,x,t) = \left(\frac{2m_t^*}{\hbar^2}\left[V_B(x,t) - E\right]\right)^{\frac{1}{2}} \tag{10}$$

Here, $V_B(x,t)$ is the x- and t-dependent potential barrier through which the electrons tunnel and m_t^* is the effective mass of the electrons in the barrier region. (In general, m_t^* can also be energy dependent.) Thus, within the WKB approximation g(E,x,t) has the general form

$$g(E,x,t) = \alpha(E,x,t)e^{-Z(E,x,t)} \tag{11}$$

where everything but the exponential decay factor is lumped into a "prefactor" $\alpha(E,x,t)$. The exponential term may loosely be thought of as controlling the penetration of the electrons into the insulator and α as being the "supply function" for the tunneling electrons, i.e., the number of electrons per unit time attempting the transition. The reason for writing g in the form of equation (11) is that except for band-edge effects--to be discussed in more detail later--the prefactor term $\alpha(E,x,t)$ is a relatively slowly varying function of both E and x as compared with the exponential. As we see below, this fact can be used to great advantage in effecting the integration of equation (4).

In order to obtain a qualitative feeling for the nature of the solution, consider a very simple case for which J(t) and Q(t) can be directly evaluated without making further approximations. Namely, we consider the case of a single trap level of energy E with uniform

spatial distribution N. Only one-dimensional tunneling is considered and the effects of the internal electric fields are neglected (valid only for small charge densities at low applied bias levels). Then α is a constant and $Z = 2\beta x$ is a function only of x with

$$\beta = \left(\frac{2m_t^*}{\hbar^2}\left[V_B - E\right]\right)^{\frac{1}{2}}$$

Direct integration of equations (4) and (5) yields

$$J(t) = \frac{N}{2\beta t}\left(1 - e^{-\alpha t}\right) \tag{12}$$

$$Q(t) = \frac{N}{2\beta}\left[E_1(\alpha t) + \ell n(\alpha t) + \gamma\right] \tag{13}$$

where $\gamma = 0.57721\ldots$ is Euler's constant and E_1 is the exponential integral defined by[6]

$$E_1(\tau) = \int_\tau^\infty \frac{e^{-\tau'}}{\tau'}\, d\tau' \tag{14}$$

The limiting forms of $E_1(\tau)$ are

$$E_1(\tau) = \begin{cases} -\gamma - \ell n\tau - \sum_{n=1}^{\infty} \frac{(-\tau)^n}{nn!} & \text{for } \tau < 1 \\ \frac{e^{-\tau}}{\tau} \sum_{n=0}^{\infty} (-1)^n \frac{n!}{\tau^n} & \text{for } \tau > 1 \end{cases} \tag{15}$$

Note in particular that $E_1(\tau)$ goes to zero rapidly for $\tau > 1$.

---

[6] *M. Abramowitz and I. A. Stegun, Handbook of Mathematical Functions, Dover Publications, Inc., New York (1965).*

Some of the main features of the results, equations (12) and (13), are as follows: The time scale of the tunneling current is set by the value of α. At early times, $t << \alpha^{-1}$, $J(t)$ and $Q(t)$ have the simple form

$$J(t) \cong \frac{N\alpha}{2\beta}\left(1 - \frac{\alpha t}{2}\right) \qquad (16a)$$

$$Q(t) \cong \frac{N\alpha t}{2\beta}\left(1 - \frac{\alpha t}{4}\right) \qquad (16b)$$

for $t << 1/\alpha$

Thus, $J(t) \to$ constant and $Q(t)$ increases linearly with t as $t \to 0$. At $t \sim \alpha^{-1}$ the form of $J(t)$ changes from that of equation (16) to an inverse time relationship, and for $\to \alpha^{-1}$ we have simply

$$J(t) \cong \frac{\cdot\cdot}{2\beta t} \qquad (17a)$$

$$Q(t) \cong \frac{N}{2\beta}\left(\ell n \alpha t + \gamma\right) \qquad (17b)$$

for $t >> 1/\alpha$

In this time regime the characteristic logarithmic dependence of the total transferred charge is obtained. If β is known then a plot of Q versus log time yields directly the trap density.

The solution to the simple case under consideration can be extended immediately to an arbitrary trap distribution in energy $N(E)$, but where the distribution still is spatially uniform. Still only one-dimensional tunneling is considered, and band bending due to internal electric fields is neglected. Here α and β become functions

of E, but there is no coupling between different values of E, so that equations (12) and (13) become simple integrals over the energy distribution

$$J(t) = \int_0^{E_c^i} dE \, \frac{N(E)}{2\beta(E)t} \left[1 - e^{-\alpha(E)t}\right] \tag{18}$$

$$Q(t) = \int_0^{E_c^i} dE \, \frac{N(E)}{2\beta(E)} \left[E_1(\alpha(E)t) + \ln(\alpha(E)t) + \gamma\right] \tag{19}$$

Note that for $t \gg 1/\alpha(E)$ for all E values of interest, the characteristic t^{-1} dependence of $J(t)$ and $\ln(t)$ dependence of $Q(t)$ is still obtained.

Before considering the integration of equations (4) and (5) for $J(t)$ and $Q(t)$ in the general case, we examine the structure of the occupied trap distribution $n(x,t)$ and the transition rate function $T(x,t)$ for the simple one-level case. This offers valuable insight on how to proceed with the general case. Substituting $g = \alpha e^{-\beta x}$ into equations (3) and (1) yields

$$n(x,t) = N\left[1 - e^{-\alpha t e^{-2\beta x}}\right] \tag{20}$$

$$T(x,t) = N\alpha e^{-2\beta x} \, e^{-\alpha t e^{-2\beta x}} \tag{21}$$

In figure 2 the normalized distribution n/N versus x is plotted at values of time spaced at order-of-magnitude intervals. Time is scaled in units of α^{-1} and x is scaled in units of $(2\beta)^{-1}$. The dashed curve simply reflects the exponential decay of the tunneling probability with x (not to scale). The important point of figure 2 is that at a given time the trap distribution is essentially saturated out to the vicinity of some point x_m (to be rigorously defined below) about which the distribution falls nearly to zero in a distance of the order of

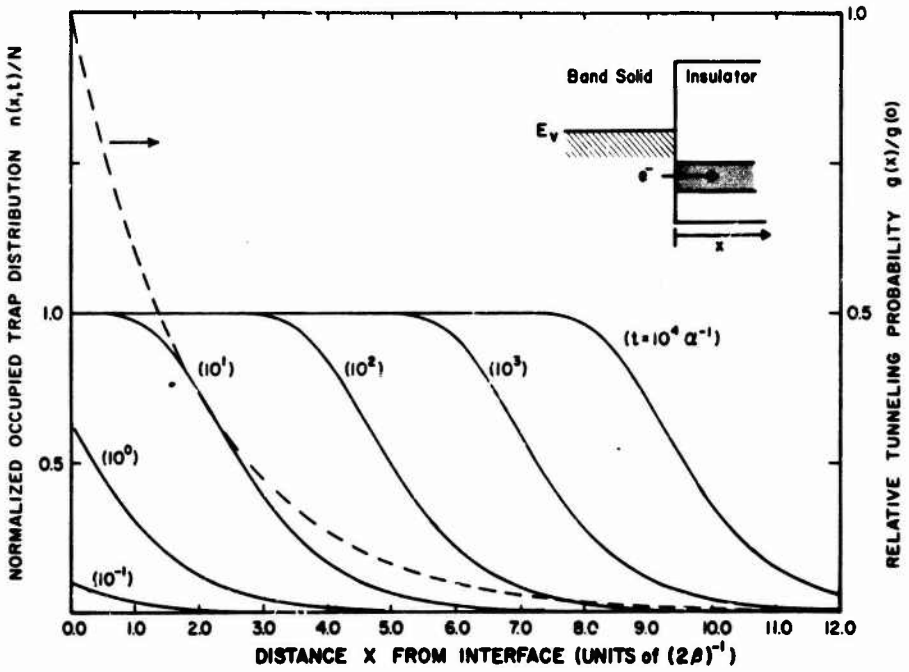

Figure 2. The normalized occupied trap distribution as a function of distance from the tunneling interface at decade increments in time for a single trap level. Time is scaled in units of α^{-1} and x in units of $(2\beta)^{-1}$. The dashed curve reflects the exponential decay of the relative tunneling probability with distance.

several scaled units. The point x_m for $t > \alpha^{-1}$ obviously increases with time in a logarithmic fashion. Since the transition rate function T(x,t) is proportional to the product of the number of unoccupied traps and the exponential decay factor, we see that T(x,t) will be peaked rather sharply in the vicinity of the fall off of the occupied trap distribution. In fact, we shall define $x_m(t)$ to be the point at which the tunneling transition rate is maximized at time t; i.e., we find x for which $\partial T(x,t)/\partial x = 0$, with the result

$$x_m(t) = \begin{cases} 0 & \text{for } t < \alpha^{-1} \\ \frac{1}{2\beta} \ln(\alpha t) & \text{for } t > \alpha^{-1} \end{cases} \tag{22}$$

This again describes the logarithmic time dependence of the total transferred charge. In fact, comparing equations (17) and (22) for $t >> \alpha^{-1}$ we see that $Q(t)$ can be written

$$Q(t) = N\left[x_m(t) + \frac{\gamma}{2\beta}\right] \tag{23}$$

The term $\gamma/2\beta$, which is of the order of 0.5 Å for typical values of β, accounts for the asymmetry of $n(x,t)$ around $x_m(t)$. For $t >> \alpha^{-1}$ the distribution $n(x,t)$ has a universal shape relative to the point $x_m(t)$ and the same is true for the profile (but not magnitude) of $T(x,t)$. Figure 3 shows the normalized distribution plotted versus $x-x_m(t)$, and also shows the profile of the transition rate about $x_m(t)$. We see that $T(x,t)$ is indeed peaked rather sharply about $x_m(t)$ with a width at half-maximum (FWHM) of three scaled units $(2\beta)^{-1}$. For the situations to be considered in the typical MIS structures, β generally

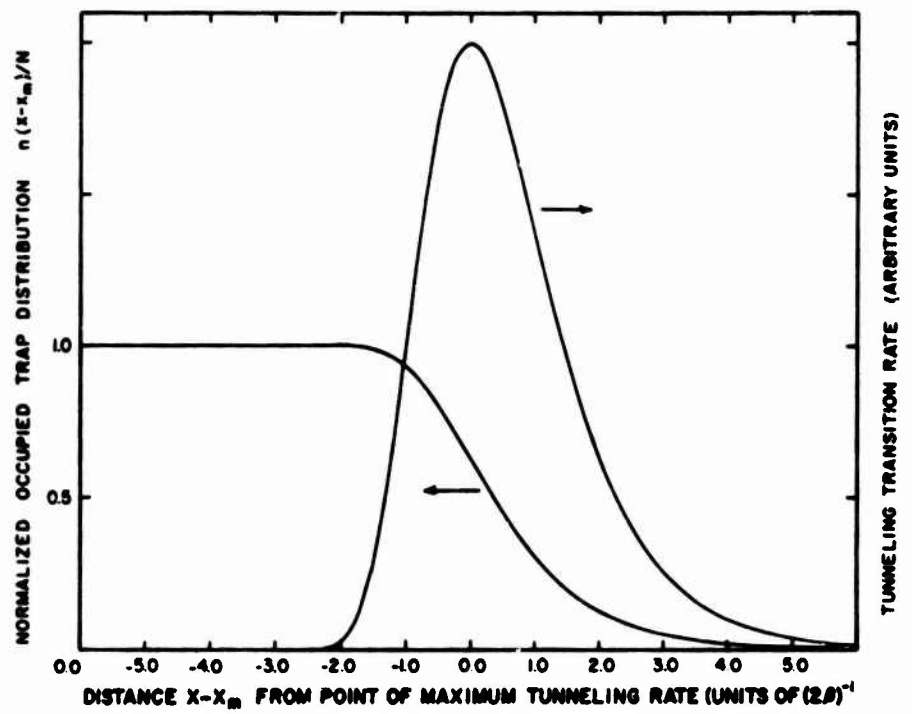

Figure 3. The normalized occupied trap distribution and relative tunneling rate plotted against distance from the point of the maximum tunneling rate.

lies in the range 0.5 to 1.0 inverse angstrom units. Hence, the full width at half maximum (FWHM) of $T(x,t)$ is of the order 1.5 to 3.0 Å. Thus, at any time t, most of the tunneling "action" is taking place to localized states lying in a narrow region of width several angstroms centered around the distance $x_m(t)$ from the interface.

3. APPROXIMATE SOLUTION IN THE GENERAL CASE

The formalism of the previous section will now be applied to the solution of the tunneling problem in the general case, namely, where we want to consider (1) the effects of internal electric fields, (2) possible spatial variations in the trap densities, (3) three-dimensional tunneling, and (4) realistic forms for the prefactor term $\alpha(E,x,t)$ of equation (11) as calculated within some model. In the general case it is not possible to obtain an analytic solution. Equations (4) and (5) must be solved numerically along with Poisson's equation, and $\alpha(E,x,t)$ in equation (11) is calculated within some reasonable approximation. However, the logarithmic dependence of the transferred charge on time is characteristic of direct tunneling into localized states and carries over generally, but with some modifications, to more complicated cases. Modifications to the $\ln(t)$ behavior are due mainly to: (1) the relaxation of the energy bands in the insulator due to the tunneled charge, which is particularly important for tunneling from states near a band edge in the semiconductor, and (2) spatial variations in the trap density in the interface region. In this last case it is possible to map out the actual spatial distribution of the trap density near the interface by analysis of the slopes of annealing or injection curves (as long as the band relaxation effects are small).

The essential point is that even in the general case, as long as the electrostatic potential, $\phi(x,t)$, and $N(E,x)$ vary sufficiently slowly, it is the exponential term in equation (11) that dominates the spatial dependence of $g(E,x,t)$ and, consequently, of $T(E,x,t)$. Therefore, the qualitative picture depicted in figure 3 is still valid. In particular, at time t the tunneling transition rate for electrons of energy E is peaked at a distance $x_m(E,t)$ with a spread around $x_m(E,t)$ of the order of several angstroms. We may take advantage of this feature by expanding all terms in the integral of equation (4) except the exponential terms, e^{-Z}, about the point $x_m(E,t)$ (keeping in mind the energy dependence of x_m), which is found by maximizing $T(E,x,t)$ with respect to x. As long as $\phi(x,t)$ and $N(E,x,t)$ vary slowly over distances of the order of ~ 3 Å, it is sufficient to retain only the first or second terms of the expansions, and the evaluations of $J(t)$ and $Q(t)$ are simplified considerably. Omitting the details of the calculations here, we give the essential results for the case where only the leading order terms in the expansions are retained. The point $x_m(E,t)$ is found to satisfy the following conditions. If $x_m^o(E)$ denotes the point that maximizes $T(E,x,t)$ at $t = 0$, then for $t < t_o(E)$, $x_m(E,t) = x_m^o(E)$, where the time $t_o(E)$ is determined by the solution of the equation

$$\int_o^{t_o} dt' g\left(E, x_m^o(E), t'\right) = 1 \tag{24}$$

For $t > t_o(E)$, $x_m(E,t)$ is found to satisfy the identity

$$\int_o^{t} dt' g\left(E, x_m(E,t), t'\right) = 1 \tag{25}$$

Differentiating equation (25) with respect to t yields a differential equation for $x_m(E,t)$

$$\frac{\partial x_m(E,t)}{\partial t} = \frac{1}{2\beta_o(E)}\, g\left(E, x_m(E,t), t\right) \tag{26}$$

where

$$\beta_o(E) = \left(\frac{2m_t^*}{\hbar^2}\left[E_c^i - E\right]\right)^{\frac{1}{2}} \tag{27}$$

Equation (26) can be simply integrated forward in time to give $x_m(E,t)$

$$x_m(E,t) = x_m^o(E) + \frac{1}{2\beta_o(E)} \int_{t_o(E)}^{t} dt' g\left(E, x_m(E,t'), t'\right) \tag{28}$$

It is important to keep track of the time arguments in equations (24) to (28). We point out that $x_m^o(E)$ may be nonzero in either of two cases: (1) In a double insulator system where there are no traps in the first insulator--that nearest to the semiconductor substrate (see below for further discussion), and (2) for energy states near a band edge of the substrate solid, where the states at the surface may be in the band gap of the semiconductor, but due to band bending by electrostatic fields, tunneling may be allowed to states deeper in the insulator.

Once $x_m(E,t)$ is determined, the tunneling current J(t) and the total transferred charge Q(t) are found by carrying out Taylor expansions about $x_m(E,t)$ and performing the integration over x in equation (4) and over t' in equation (5) analytically. The results in the general case can be expressed in a form analogous to

equations (12) and (13) for the simple case considered earlier (one energy, one-dimensional tunneling, no band bending). We define a scaled time parameter $\tau(E,t)$.

$$\tau(E,t) = h(E,t)\exp\left\{\frac{2\beta_o(E)}{N\left(E,x_m\right)} \int_{x_m^o(E)}^{x_m(E,t)} dx N(E,x)\right\} \tag{29}$$

where

$$h(E,t) = \int_o^t dt' g\left(E,x_m(E,t),t'\right) \tag{30}$$

Note $h(E,t) = 1$ for $t > t_o(E)$ by the identity (eq (25)). In terms of the scaled time $\tau(E,t)$, $J(t)$ and $Q(t)$ can be expressed as

$$J(t) = e\int dE \frac{N\left(E,x_m\right)}{2\beta_o(E)} \frac{g\left(E,x_m,t\right)}{h(E,t)} \left[1 - e^{-\tau(E,t)}\right] \tag{31}$$

$$Q(t) = e\int dE \frac{N\left(E,x_m\right)}{2\beta_o(E)} \left[E_1(\tau) + \ln(\tau) + \gamma\right] \tag{32}$$

where $x_m = x_m(E,t)$ and $\tau = \tau(E,t)$ are understood.

Of course, the tunneling equations (24) to (32) are to be solved simultaneously with Poisson's equation. However, we again take advantage of the nature of the occupied trap distribution as shown in figure 2. Namely, it is a good approximation to assume that at time t traps of energy E are essentially saturated to the point $x_m(E,t)$ and empty beyond. Then an analytical solution to $\phi(x,t)$ in terms of a simple quadrature over E can be effected. Let $\phi_o(x)$ be the electrostatic potential at $t = 0$, which is determined by the applied bias, work function difference, image potential, and the initial

charge distribution in the insulator. We assume that the change in the potential with time is due solely to the tunneled charge. Then, at time t,

$$\phi(x,t) = \phi_o(x) - \frac{1}{C_i} Q(t) \frac{x}{\ell_i} + \frac{e}{\epsilon_i} \int d\bar{E} \bar{N}(E,t) F\left(x; x_m^o(E), x_m(E,t)\right) \tag{33}$$

where

$$\bar{N}(E,t) = \frac{1}{x_m(E,t) - x_m^o(E)} \int_{x_m^o(E)}^{x_m(E,t)} dx N(E,x) \tag{34}$$

and

$$F\left(x; x_1, x_2\right) = \begin{cases} 0 & \text{for } x < x_1 \\ (1/2)\left(x - x_1\right)^2 & \text{for } x_1 < x < x_2 \\ \left(x_2 - x_1\right)\left(x - \frac{x_1 + x_2}{2}\right) & \text{for } x > x_2 \end{cases} \tag{35}$$

with $x_2 > x_1$. Also in equation (33), $C_i = \epsilon_i/\ell_i$ is the insulator geometrical capacitance, where ϵ_i is the insulator dielectric constant, and ℓ_i is the insulator thickness.

By taking advantage of the peaked structure of $T(E,x,t)$ around $x_m(E,t)$, we have been able to transform the general solution to the tunneling problem, equations (4) and (5), into a form directly amenable to numerical calculation. One simply integrates equation (28) forward in time in conjunction with simple quadratures over energy. All that remains is to determine an appropriate form for the Green's function, $g(E,x,t)$, or more to the point, determine an appropriate form for the prefactor $\alpha(E,x,t)$ in equation (11). We have not carried out a complete quantum-mechanical calculation, but we have calculated g within a semiclassical treatment that contains all the salient features of a more rigorous treatment. In particular, our

treatment includes the density of states of the semiconductor (therefore band-edge effects are included) and accounts for three-dimensional effects. We take the electrons within a band in the semiconductor to be simulated by a free electron gas with an effective mass m^* appropriate to the band electrons. We treat the electrons striking the boundary as particles having a WKB probability factor $e^{-\kappa}$ for penetration into the barrier region $x > 0$, which is weighted according to the normal component of the electron velocity v_x in the manner

$$\kappa(E,x,t) = \frac{v}{v_x} Z(E,x,t) \tag{36}$$

where $Z(E,x,t)$ is given by equation (9) and v is the total electron velocity. This weighting procedure simulates the more rigorous, but much more complicated, quantum mechanical result[5] in which electrons striking the surface at near-normal incidence have a much larger penetration probability to a distance x than those with an appreciable velocity component parallel to the surface. For electrons of energy E the calculation of g involves a summation over all possible wave vectors having a positive x component. We give the final result for elastic tunneling of electrons from the semiconductor valence band, taken to be isotropic, to a localized trap of energy E located at a distance x from the interface

$$g(E,x,t) = \frac{2\pi m^*}{(2\pi\hbar)^3} \sigma(E)\theta(E')E'F(Z)e^{-Z} \tag{37}$$

[5] *C. B. Duke, Tunneling in Solids, Academic Press, New York (1969), p. 30.*

where

$$E' = E_v - E + \phi(x,t) \tag{38}$$

$$\theta(E') = \begin{cases} 1 & \text{for } E' > 0 \\ 0 & \text{for } E' < 0 \end{cases} \tag{39}$$

$$Z = 2x\left[\frac{2m_t^*}{\hbar^2}\left(E_c^i - E + \frac{\phi(x,t) - \phi(0,t)}{2}\right)\right]^{1/2} \tag{40}$$

$$F(Z) = (1/2)\left[1 - Z + e^{Z}E_1(Z)\right] \tag{41}$$

and $\sigma(E)$ is an effective capture cross section per unit energy for the traps of energy E and has to be determined by comparison with experimental data. The m^* appearing in equation (37) is appropriate for the semiconductor valence band and the m_t^* in equation (40) is that appropriate for electrons in the potential barrier region. For multiple overlapping valence bands--as in the case for Si--the m^* in equation (37) is simply replaced by a sum over the m^* for each band. The function F(Z) accounts for the three-dimensional effects; it has the limiting forms

$$F(Z) \doteq \begin{cases} 1/2 & \text{for} \quad Z \to 0 \\ (1/Z)\left(1 - \frac{3}{Z}\right) & \text{for} \quad Z \gg 1 \end{cases} \tag{42}$$

For trap states near the interface, essentially all electrons in the hemisphere for $v_x > 0$ contribute equally to the tunneling probability, whereas for states far removed from the interface, only those electrons striking the surface with near-normal incidence contribute significantly to the tunneling. This decrease in the number of effective electrons is reflected in the Z^{-1} dependence of F(Z) for large Z. In writing equation (40) we have assumed that $\phi(x,t)$ can be

approximated by a straight line in the insulator. However, this linear approximation--being made within the square root--introduces little error as long as $\phi(x,t)$ is reasonably smooth and the total change in ϕ in the tunneling region is not comparable to the magnitude of $E_c^i - E$, which is assumed to be true for our present applications.

The result for $g(E,x,t)$ has been given for electrons tunneling from the valence band of the semiconductor. Analogous results hold for electrons tunneling from the conduction band as well as for tunneling at the metal insulator surface. The results can also be extended to include tunneling from an anisotropic band described by an effective mass $m_\perp^*$ for electron wave vectors normal to the interface and by an effective mass $m_{\parallel}^*$ for electron motion parallel to the interface. The essential result for the case $Z >> 1$ is that the m^* of equation (37) is replaced by $m_\perp^*(m_{\parallel}^*/m_\perp^*)^2$. For the conduction band of silicon oriented in the 100 direction this leads to a reduction in the tunneling rate by a factor of ~100.

The theory has been developed explicitly for situations for only a single insulator. But the theory is readily extended to the double insulator system, as is thought to be the situation for Al_2O_3 MIS devices where a thin intermediary SiO_x layer of width 10 to 30 Å lies between the Si substrate and the Al_2O_3 insulator film. We assume that trapping states in the intermediary film are unimportant and that tunneling occurs from the band states of the semiconductor through the intermediary film and into localized states in the second insulator film. If x_o is the width of the intermediary film and the coordinate

system is located so that x = 0 refers to the interface between the two insulators, so that $N(E,x) \neq 0$ only for $x > 0$, then equation (37) becomes

$$g(E,x,t) = \frac{2\pi m^*}{(2\pi\hbar)^3}\,\sigma(E)\theta(E')E'F\left(Z + Z_o\right)e^{-\left(Z + Z_o\right)} \tag{43}$$

where

$$Z_o = 2x_o\left[\frac{2m_t^*}{\hbar^2}\left(E_c^i - E + \phi(x,t) - \frac{\phi(o,t)}{2}\right)\right]^{\frac{1}{2}} \tag{44}$$

In Z_o, m_t^* and E_c^i refer to the tunneling effective mass, and conduction band edge, respectively, of the intermediary insulator, whereas in equation (40) for Z they refer to those quantities in the second insulator. Also, in expression (33) for the electrostatic potential, a term

$$-\frac{\varepsilon_2}{\varepsilon_1}\,\mathcal{E}_o(t)\,x_o$$

must be added to account for the potential drop across the intermediary film. Here, $\mathcal{E}_o(t)$ is the electric field just inside the second insulator and the ratio $\varepsilon_2/\varepsilon_1$ of the dielectric constants of the two insulators accounts for the discontinuity at the boundary x = 0 between the two (different) dielectric media.

4. MODEL CALCULATIONS

In this section model calculations will be presented based on the numerical solution of the tunneling equations developed in the previous section. These calculations are for relatively simple model

systems in order to exhibit the major features and predictions of the theory. A detailed comparison of the model with charge injection data on Al_2O_3 MIS capacitors has been described elsewhere.[1]

The model systems used in the calculations were chosen to be representative of several cases important in practice. First, the field injection characteristics of Al_2O_3 MIS capacitors are calculated for two cases: one in which a thin SiO_2 layer is present between the Si substrate and the deposited Al_2O_3 film, and the other in which there is no SiO_2 layer present. The energy band diagrams for these two cases are depicted schematically in figure 4 for zero and positive applied bias conditions. The energy positioning of the

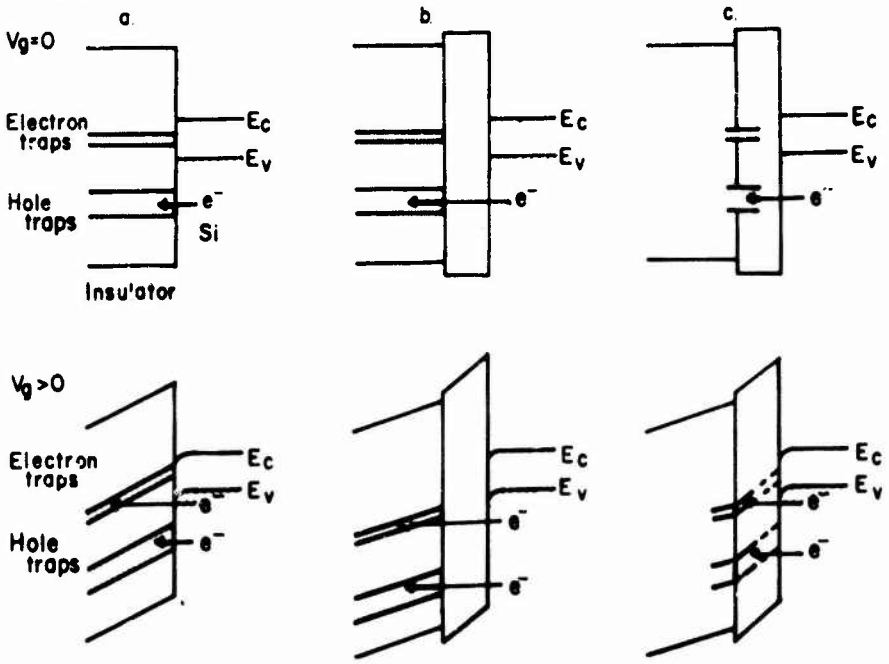

Figure 4. Schematic energy band diagrams for model calculations (top diagrams: flat band condition; bottom diagrams: positive applied bias); (a) single-insulator system, (b) double-insulator system--localized traps associated with second (extended) insulator, and (c) double-insulator system--traps associated with intermediate insulator or with interface region between two insulators.

[1] *F. B. McLean, H. E. Boesch, Jr., P. S. Winokur, J. M. McGarrity, and R. B. Oswald, Jr., IEEE Trans. Nucl. Sci. NS-21 (1974), 47.*

electron trap band (to be discussed in more detail below), is such that at flat-band conditions the electron traps have energies lying opposite to the forbidden gap of the silicon substrate (top diagrams in fig. 4). When positive bias is applied to the MIS structure, these states shift down in energy relative to the Si bands, and for sufficiently large bias, direct tunneling will occur into them from the Si valence band (bottom diagrams of fig. 4). Finally, the charge relaxation characteristics following irradiation are calculated due to tunneling of electrons into the insulator and recombining with a trapped hole distribution in the interface region. This case is also depicted schematically in figure 4. The hole traps are assumed to have energies which at flat-band conditions are below the Si valence band edge. Though normally unoccupied, these states become populated by capturing holes generated by ionizing radiation. Holes trapped sufficiently close to the interface subsequently can serve as receptor states for electrons tunneling from the Si valence band. This tunneling/recombination process may be an important mechanism for the annealing of radiation-induced positive charge at the Si interface in both Al_2O_3 and SiO_2 MIS devices. In the calculations presented here, emphasis is placed upon the effects produced by spatial variation of the trapped hole distribution. In certain instances it may be possible to profile the spatial distribution of the trap density near the interface by appropriate analysis of experimental data.

The primary input to the numerical calculations is the spatial and energy distribution of the insulator trap states. For the calculations reported here, the energy and spatial distributions are assumed to be separable, i.e., $N(E,X) = N(E)f(x)$. The energy distribution $N(E)$ is taken to be gaussian, and the spatial distribution $f(x)$ to be an analytic form that is integrable in expressions such as equations (29) and (34). The calculations proceed by the integration of equation (28) for $X_m(E,t)$ forward in time along

with the integral of Poisson's equation, equation (33), and utilizing equations (37) to (41) describing the form of the Green's function g(E,x,t) employed here. Once X_m (E,t) is known, equation (29) is evaluated for the scaled time parameter τ(E,t), along with the function h(E,t). Then the tunneling current J(t) and accumulated charge Q(t) are calculated by simple integrations over the trap energy distribution with equations (31) and (32). For the double insulator case the modifications described at the end of section 4 are used. We now discuss the results of the representative model calculations.

4.1 Field-Injection Characteristics

We first present the model calculations of field-injection characteristics for several cases appropriate to Al_2O_3 MIS systems, assuming that direct tunneling is the mechanism at work. As mentioned earlier, for the modeling we consider a band of electron traps which at flat-band conditions lies adjacent to the forbidden gap of the Si substrate. This configuration was chosen on the basis of photodepopulation data presented by Harari and Royce[7] which indicated that such a band (their so-called "c" band) is a major recipient of field-injected electrons. Further, photodepopulation studies carried out on samples used in a previous HDL study[1] indicate that at room temperature and for bias levels up to about 25 V above the flat-band voltage, almost all the field-injected electrons ended up in states in this same energy region. In general, other electron trap levels may come into play and perhaps other processes, particularly at higher bias levels where tunneling from the Si conduction band into higher trap levels, or into the insulator conduction band is possible. Nevertheless, the essential features of the field-injection charac-

---

[1] *F. B. McLean, H. E. Boesch, Jr., P. S. Winokur, J. M. McGarrity, and R. B. Oswald, Jr., IEEE Trans. Nucl. Sci. NS-21 (1974), 47.*

[7] *E. Harari and B. S. H. Royce, IEEE Trans. Nucl. Sci. NS-20 (1973), 280.*

teristics can be extracted based upon the following simple idea. This band of electron traps is nearly empty at flat-band conditions due to the unavailability of electrons for direct tunneling into them, but as positive bias is applied the band bends downward with respect to the Si band structure (see fig. 4a and 4b). At sufficiently high bias, direct tunneling is possible from the Si valence band into the localized electron states in the insulator. This idea forms the basis for the theory behind a certain class of MNOS memory transistors.*

In particular, for our model calculations we consider a trap band of uniform spatial density of 5.0×10^{19} cm^{-3} (based on experimental data[1]), but having a gaussian energy distribution peaked at flat-band condition at an energy of 0.6 eV above the Si valence band edge and with a FWHM of 0.2 eV.[7] The Si valence band edge is located 4.1 eV below the Al_2O_3 insulator conduction band. The total oxide thickness is taken to be 1000 Å, and the effective mass of the tunneling electrons is taken as 0.4 times the free electron mass.[8]

Figure 5 presents the field-injection curves appropriate for a double insulator situation where a thin SiO_2 film 20 Å thick is postulated to exist between the Si substrate and the extended Al_2O_3 insulator. This is thought to be the case by many

*See Annotated Bibliography, Theory of MNOS Memory Transistors.

[1] F. B. McLean, H. E. Boesch, Jr., P. S. Winokur, J. M. McGarrity, and R. B. Oswald, Jr., IEEE Trans. Nucl. Sci. NS-21 (1974), 47.

[7] E. Harari and B. S. H. Royce, IEEE Trans. Nucl. Sci. NS-20 (1973), 280.

[8] M. Lenzlinger and E. H. Snow, J. Appl. Phys. 40 (1967), 278.

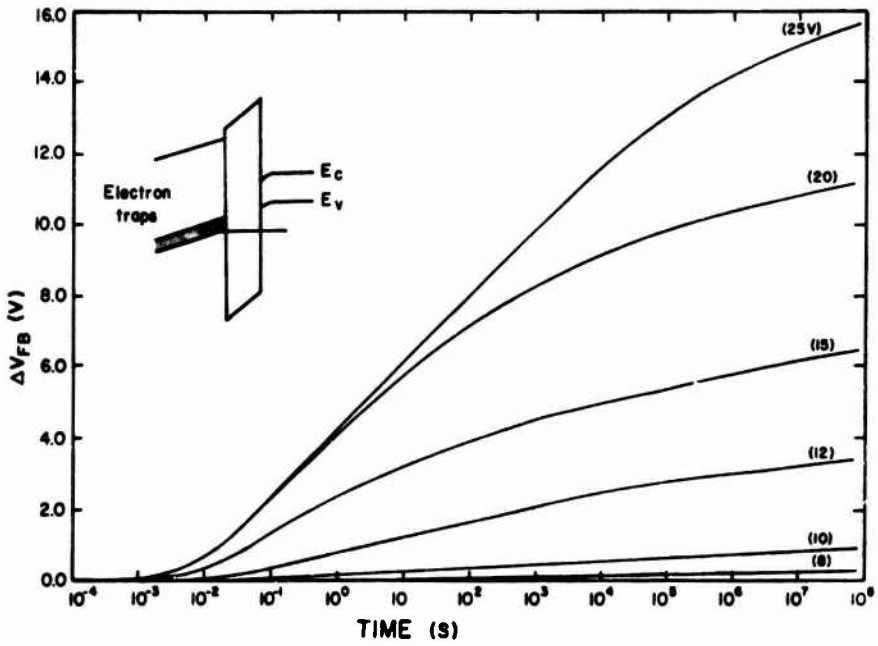

Figure 5. Model calculations of field injection, ΔV_{FB} versus time, for double-insulator MIS system with 20-Å SiO_2 film between Si substrate and extended Al_2O_3 insulator. Electron trap density = 5.0×10^{19} cm^{-3}, electron trap band width = 0.2 eV, and mean energy is 0.6 eV above Si valence band (applied bias for each curve shown in parentheses).

investigators[7] when Al_2O_3 is directly deposited onto a Si substrate. Here we assume that the electron traps are associated with the Al_2O_3 insulator material. Figure 5 shows the shift in flat-band voltage ($\Delta V_{FB}(t) \propto Q(t)$) versus time after application of positive bias for a series of bias voltages (indicated by the numbers in parentheses). Noticeable injection begins at a bias level of about 8 V relative to flat band, and the injection rapidly picks up with

[7] *E. Harari and B. S. H. Royce, IEEE Trans. Nucl. Sci. NS-20 (1973), 280.*

increasing bias. We note that the injection is effectively controlled by the intermediate SiO_2 film; it is the potential drop across this film which sets the injection threshold. Further, the time scale for tunneling is controlled by its thickness; as a consequence the injection curves for all bias levels begin (on a log scale) at about the same time. The other general feature to note here is that the injection curves initially break into the characteristic ln(t) behavior, but as time progresses they tend to flatten out (especially evident at the higher bias levels). This apparent saturation effect is a direct consequence of the relaxation of the bands due to the tunneled charge, and this relaxation is amplified across the thin SiO_2 film due to the difference in dielectric constants of Al_2O_3 and SiO_2. (We take the relative dielectric constant to be 3.85 for SiO_2 and 8.5 for Al_2O_3.)

Figure 6 shows the injection curves for a single insulator situation; a similar trap structure as in the previous case is considered, but the thin SiO_2 film is omitted. Now, within our model

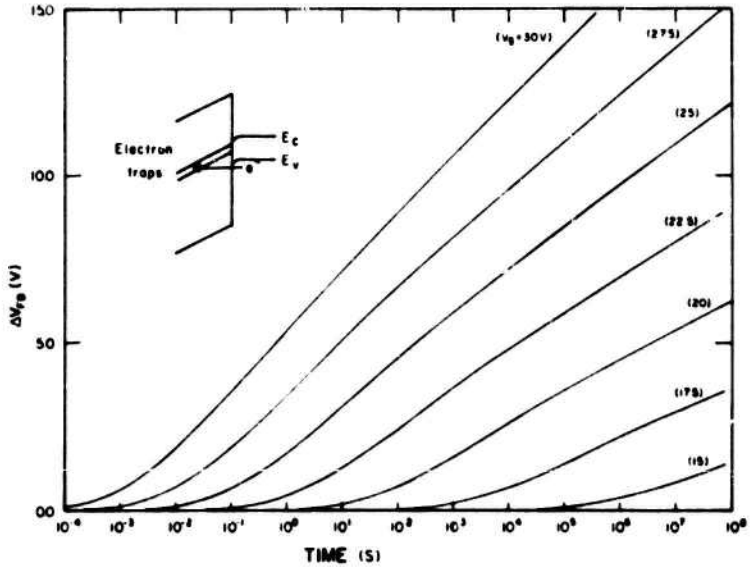

Figure 6. Calculated field-injection characteristics for single-insulator MIS system. The same electron trap parameters were used as those in figure 5.

the initial tunneling rate is determined by the position of the closest available states for direct tunneling from the Si valence band, and for this case this distance is inversely proportional to the electric field at the interface. As the field is increased the insulator energy bands bend downward more sharply and this distance decreases (see fig. 4a), leading to an increased initial tunneling rate. Consequently, as the bias is increased the injection curves begin breaking into the ln(t) behavior at increasingly earlier times. Other points to note are that the slopes of the curves in the log regime are nearly parallel (but with some fanning out evident) and that the relaxation effect due to the tunneled charge is considerably reduced because of the absence of the intermediate SiO_2 film of lower dielectric constant.

Figure 7 shows the calculated bias-stress curves for the single and double insulator cases where the flat-band shift 10^3 s after application of the bias is plotted versus the applied bias. Both curves exhibit a pronounced threshold for injection, as is observed

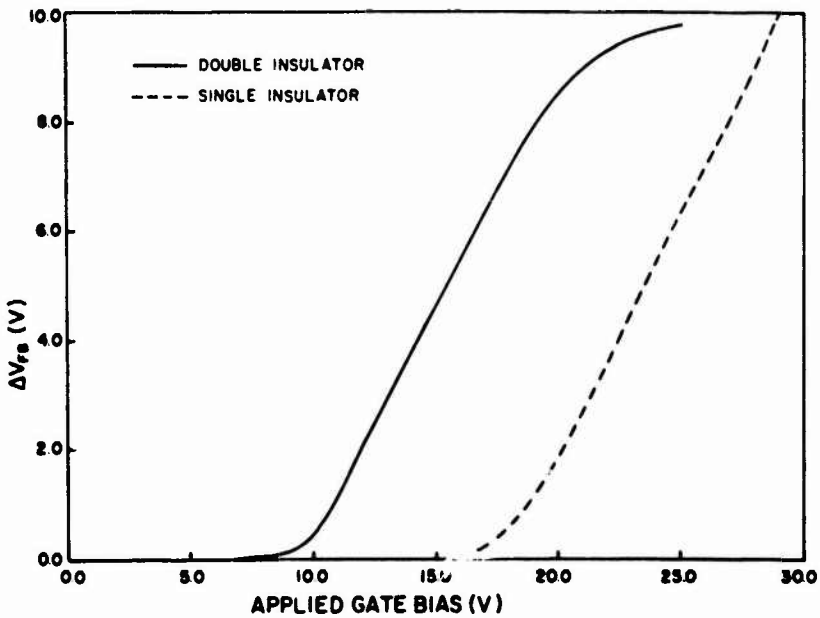

Figure 7. The calculated flat band voltage shift after application of bias for 1000 s plotted versus applied gate bias for the single- and double-insulator model systems.

experimentally. The threshold voltage bias is considerably smaller for the double insulator system (for the model parameters used in the present calculations) than for the single insulator. This can be directly attributed to the enhanced potential drop (or band bending) across the intermediate film as a result of the mismatch in dielectric constants, thereby producing smaller values of $X_m^o(E)$ in the double insulator system. This would no longer be the case at sufficiently high bias levels where $X_m^o < 20$ Å for the single insulator system, but this occurs outside the bias range considered here. The other major qualitative feature distinguishing the two cases is that there is a "slowing down" of the field injection at the higher bias levels for the double insulator case as compared with the bias-stress curve for the single insulator, where strong injection continues with increasing bias. The difference again can be attributed to the more pronounced relaxation effect in the double insulator system.

Next, we discuss the effect of the trap bandwidth on the injection characteristics for the single insulator. In figure 6, where the bandwidth is taken to be 0.2 eV, the transition region from the initial flat slope (on a log plot) to the logarithmic regime is relatively narrow. However, if the bandwdith is increased to 0.6 eV, as for the injection characteristics shown in figure 8, this transition region is broadened considerably. This broadening is due basically to the increased spread in the closest states available for direct tunneling between the top and bottom of the electron trap band. In practice, by appropriate analysis of the injection curves for this case, information can be obtained concerning the energy structure of the trap band. To see this, refer to figure 9, where at flat-band conditions the bottom and top of the trap band are taken to be Δ_1 and Δ_2, respectively, relative to the Si valence band edge. The transition time t_1 is defined as the time at which a noticeable flat-band shift due to the injection process is first obtained; it corresponds approximately to the time at which a significant quantity of electrons have tunneled into the nearest

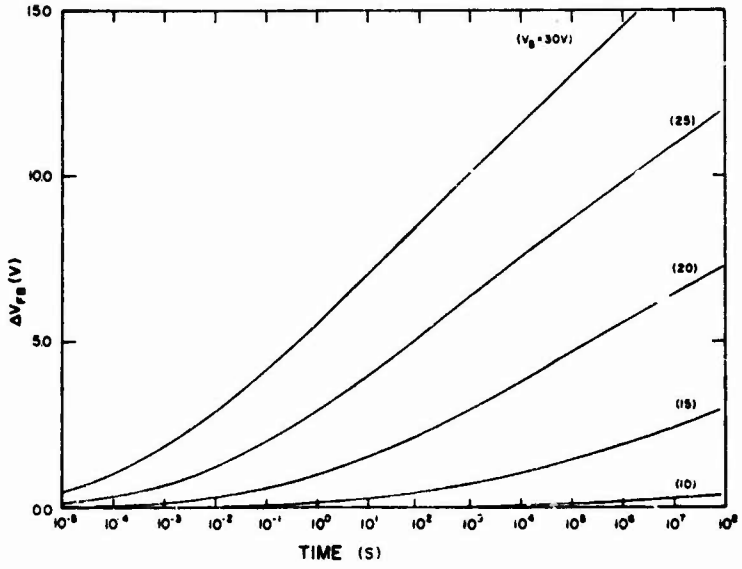

Figure 8. Calculated field-injection characteristics for a single-insulator MIS system illustrating the effect of increased electron trap band width (0.6 eV).

ANALYSIS OF INJECTION CURVE: SINGLE INSULATOR

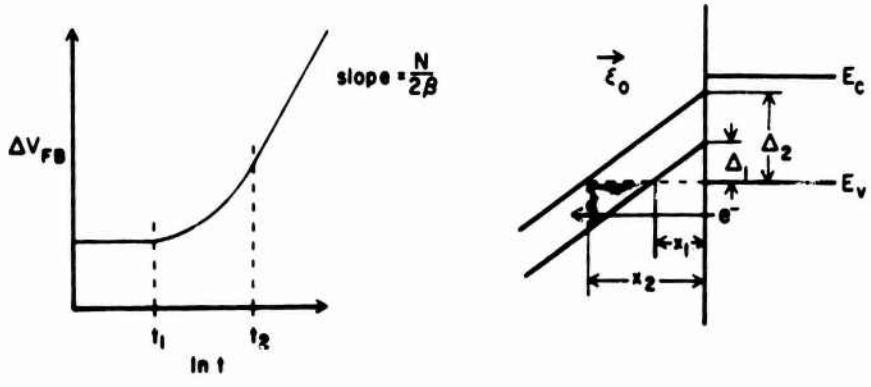

$$\ln (t_i/t_0) = 2\beta x_i = 2\beta\Delta_i / \mathcal{E}_0$$

Figure 9. Determination of electron trap band parameters from a typical experimental injection-dominated transient flat band voltage response curve.

available states for tunneling (at x_1). These states are associated with the lower edge of the trap band (at Δ_1). The second transition time, t_2, is defined as the time at which the injection curve approaches true logarithmic behavior. It corresponds to the time at which the

closest available states (at x_2) or traps near the upper edge of the trap band (at Δ_2) have become saturated, and after which the tunneling transition rate to all energy levels in the band decays as t^{-1} (and hence ΔV_{FB} increases as $\ln(t)$). Now, within the WKB approximation the characteristic tunneling time t_i to states located Δ_i above E_v at flat-band conditions is given by $t_i = t_i^o \exp(2\beta x_i)$ where β is an averaged value of the WKB integrand (eq (9)) over the energy range of concern, and x_i is the distance required for the electrostatic potential to change by an amount Δ_i from its value at the interface. Since $x_i = \Delta_i/\mathcal{E}_o$ where $\mathcal{E}_o$ is the electric field in the interface region, the expression for t_i can be rewritten as

$$\ln \frac{t_i}{t_i^o} = 2\beta\Delta_i/\mathcal{E}_o \ . \tag{45}$$

Hence, an estimate of the values of Δ_1 and Δ_2 can be obtained by plotting the log of t_1 and t_2 versus $\mathcal{E}_o^{-1}$. The intercepts of such plots at $\mathcal{E}_o^{-1} = 0$ can be used to obtain estimates of the capture cross sections of the traps.[1]

To conclude this section we note the injection characteristics computed by using the direct tunneling model are qualitatively different for the single and double insulator systems, and in practice it should be readily apparent which case one is observing. However, if one is dealing with a double insulator system where the electron traps, instead of being associated with the extended insulator as in figure 5, are in fact associated with the intermediate film (see fig. 4c), then the qualitative features of the injection characteristics would correspond to that of the single insulator situation, as shown in figures 6 and 8. A more subtle analysis is then required to distinguish between the cases.

---

[1] *F. B. McLean, H. E. Boesch, Jr., P. S. Winokur, J. M. McGarrity, and R. B. Oswald, Jr., IEEE Trans. Nucl. Sci. NS-21 (1974), 47.*

4.2 Post-Irradiation Charge Relaxation

Here are discussed the model calculations of rapid annealing via tunneling/recombination into a single band of trapped holes near the Si interface following a pulse of ionizing radiation. The energy levels of the trapped hole states are taken to be adjacent to the Si valence band. In particular, the peak of the band is taken to lie 1.8 eV below the Si valence band edge with a FWHM of 0.6 eV, which are reasonable values based on photodepopulation studies.[7,9] We restrict our attention to the single insulator case (of thickness 1000 Å), since the annealing characteristics are qualitatively similar where a thin intermediate insulator film is present, the only important difference being a shift in the onset time for significant tunneling. We use values for the tunneling effective mass and dielectric constant appropriate to that of SiO_2 ($m_t^* = 0.4\ m_e$, $\varepsilon_i = 3.85$). It is assumed that after the MIS capacitor has been subjected to the pulse of ionizing radiation the hole trap band is saturated in the vicinity of the interface to a distance beyond tunneling range with a resulting flat-band shift of -10.0 V. The focus of attention here is the manner in which spatial variations in the trapped hole distribution affect the annealing characteristics. To illustrate the effect we assume a simple exponential form for the spatial dependence of the distribution near the interface:

$$N(x) = N_o e^{\lambda x} \tag{46}$$

where N_o is the density of traps at the interface (integrated over all energies). We take $N_o = 2 \times 10^{19}\ cm^{-3}$, a typical value estimated from experimental data.

---

[7] *E. Harari and B. S. H. Royce, IEEE Trans. Nucl. Sci. NS-20 (1973), 280.*

[9] *E. Harari, S. Wang and B. S. H. Royce, J. Appl. Phys., 46 (1975), 1310.*

Figure 10 shows the annealing curves for several values of λ from 0.1 to -0.2 in units of 2β (β being evaluated at the peak of the trap band). Clearly, the annealing reflects directly the spatial variation of the hole distribution. This is a direct consequence of the nature of the tunneling/recombination process, namely, that there is a distinct tunneling "front" $x_m(t)$, which moves into the insulator as log time, with the states behind the front filled and those beyond it still empty. At a time t the tunneling takes place predominantly to traps located within a few angstroms of $x_m(t)$, and hence reflects the density of traps in that region. (Recall fig. 2 and 3.) More specifically, it is the slope of the annealing curve which is directly proportional to the density of traps. Hence, for a constant spatial density ($\lambda = 0.0$) the annealing curve is very nearly linear with log(t) for $t > \alpha^{-1}$. For nonzero values of λ the initial annealing behavior is very similar to

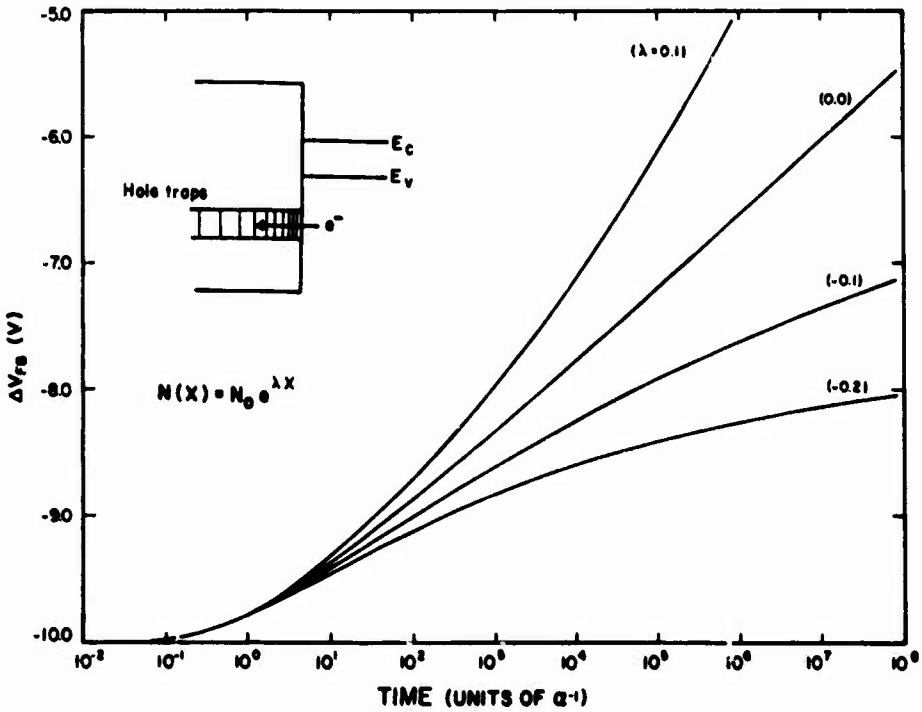

Figure 10. Calculated annealing curves, showing effect of spatial variation in traps distributions. Time is in units of α^{-1} and distance in units of $(2\beta)^{-1}$.

the constant density case, but with increasing time the slopes of the curves increase or decrease reflecting either an increasing or decreasing trap density away from the interface.

Therefore, if it is certain that the tunneling/recombination mechanism is responsible for charge annealing, the spatial profile of the trapped hole distribution near the interface can be obtained by simple analysis of the experimental annealing curves, provided that the variation of the tunneling rate with energy over the trap bandwidth is sufficiently small. This is the situation for the present model calculations for which the energy levels of the hole traps are located well into the Si valence band, and therefore the exponential WKB spatial decay factor dominates the transition rate. If the trap band were located near a band edge of the substrate, this would no longer be true as there is then a strong variation with energy in the density of electrons available for tunneling. The tunneling "front" would then be smeared out over a considerable range due to the energy dependence of $X_m(t)$, and the annealing curves would no longer be simply related to the spatial density of traps. By the same token there is little bias dependence in the annealing characteristics shown in figure 10 for the present model system. However, if the trap band were near a Si band edge, a strong bias dependence of the annealing would exist similar to the strong bias dependence of the field-injection characteristics discussed earlier.

5. SUMMARY

A general model of charge transfer at the insulator-semiconductor interface has been described. The model is based upon direct WKB tunneling of electrons from the semiconductor substrate into localized trap states in the insulator. Advantage was taken of the strong spatial

decay of the tunneling transition probability to obtain valid approximate solutions of the tunneling equations. These solutions are of a form directly amenable to numerical evaluation in cases where there is a distribution of the localized insulator states both in energy and in space. The effects of internal electric fields in the insulator are included self-consistently by solving Poisson's equation along with the tunneling equations. The results of several model calculations representative of systems important in practice were described. Some of the important points discussed are:

(a) The direct tunneling of electrons into trap states in the insulator yields the generally observed log time feature of charge transfer characteristics.

(b) The slopes of the charge transfer curves in the logarithmic regime are proportional to the spatial density of the traps.

(c) Spatial variations in the trap densities modify the log(t) dependence.

(d) The field-injection characteristics are qualitatively different for single and double insulator systems.

(e) A detailed analysis of the field-injection curves can yield information on the energy distribution of the traps.

In a recent publication, the direct tunneling model was applied in some detail to the analysis of field-injection data in Al_2O_3 MIS capacitors.[1] It was shown that electron injection under positive bias

[1] *F. B. McLean, H. E. Boesch, Jr., P. S. Winokur, J. M. McGarrity, and R. B. Oswald, Jr., IEEE Trans. Nucl. Sci. NS-21 (1974), 47.*

(as well as trapping of radiation-generated holes) is dominated by an interface transition region at the Si-Al_2O_3 interface. The extent of this region from the Si substrate as inferred from the data is of the order of 25 Å. The field injection characteristics were qualitatively explained by direct tunneling from the Si valence band into electron traps in a single insulator. Quantitative consistency between the single insulator model and the results of photodepopulation measurements after field injection was obtained if it was assumed that the dielectric properties of the transition region were similar to that of the SiO_2, and further that the electron traps were associated with the transition region rather than being situated in the Al_2O_3. Thus, the application of the model in this case led to an improved understanding of the nature of the interface region and of the factors invovled in the field-injection process.

A detailed application of the direct tunneling model to charge annealing after irradiation has not yet been undertaken. There is recent experimental evidence[2,3] in SiO_2 MIS capacitors that indicates that the dominant factor in the charge relaxation of that system is a slow, temperature-activated transport of the radiation-generated holes through the insulator to the Si interface where most of the holes (~90 percent) pass on to the substrate. The remaining fraction of holes, however, appears to be trapped near the interface. A tunneling/recombination mechanism involving these trapped holes may be responsible for the long-term annealing process observed to occur in these samples for hours or even days after the irradiation. It is planned to investigate the long-term annealing in some depth.

---

[2] *F. B. McLean, G. A. Ausman, Jr., H. E. Boesch, Jr., and J. M. McGarrity, J. Appl. Phys. 49 (1976), 1529.*

[3] *H. E. Boesch, Jr., F. B. McLean, J. M. McGarrity, and G. A. Ausman, Jr., IEEE Trans. Nucl. Sci. NS-22 (1975), 2163.*

ACKNOWLEDGEMENT

The author expresses appreciation to William Scharf for his assistance with the numerical calculations.

ANNOTATED BIBLIOGRAPHY

Charge Injection and Post-Irradiation Rapid Annealing in MOS Devices

Balk, P. and Stephany, F., J. Electrochem. Soc. 118 (1971), 1634.

Micheletti, F. B. and Kolondra, F., IEEE Trans. Nucl. Sci. NS-18 (1971), 131.

Simons, M. and Hughes, H. L., IEEE Trans. Nucl. Sci. NS-18 (1971), 106, and NS-19 (1972), 282.

Tsujide, T., Nakanuma, S. and Ikushima, Y., J. Electrochem. Soc. 117 (1970), 703.

Walden, R. H. and Strain, R. J., Proc. IEEE Reliability Symposium 23, Las Vegas (1971).

Theory of MNOS Memory Transistors

Ross, E. C. and Wallmark, J. T., RCA Rev. 30 (1969), 366.

Wallmark, J. T. and Scott, J. H., RCA Rev. 30 (1969), 335.

Theory of Frequency Response of Surface States

Heiman, F. P. and Warfield, G., IEEE Trans. ED-21 (1965), 167.

Kar, S. and W. E. Dahlke, Solid State Electronics 15 (1972), 221.

Katsube, T. and Adachi, Y., Jpn J. Appl. Phys. 12 (1973), 320.

Katto, H., and Sah, C. T., Phys. Stat. Solids (A) 13 (1972), 417.

DISTRIBUTION

COMMANDER
US ARMY MATERIEL DEVELOPMENT
& READINESS COMMAND
500 EISENHOWER AVENUE
ALEXANDRIA, VA 22333
ATTN DRXAM-TL, HQ TECH LIBRARY

COMMANDER
USA RSCH & STD GP (EUR)
BOX 65
FPO NEW YORK 09510
ATTN LTC JAMES M. KENNEDY, JR.
CHIEF, PHYSICS & MATH BRANCH

COMMANDER
USA ARMAMENTS COMMAND
ROCK ISLAND, IL 61201
ATTN AMSAR-ASF, FUZE DIV
ATTN AMSAR-RDF, SYS DEV DIV - FUZES

COMMANDER
USA MISSILE & MUNITIONS CENTER & SCHOOL
REDSTONE ARSENAL, AL 35809
ATTN ATSK-CTD-F

DIRECTOR
DEFENSE COMMUNICATIONS AGENCY
WASHINGTON, DC 20305
ATTN CODE 930, MONTE I. BURGETT, JR

DEFENSE DOCUMENTATION CENTER
CAMERON STATION
ALEXANDRIA, VA 22314
ATTN TC-TCA, (12 COPIES)

DIRECTOR
DEFENSE INTELLIGENCE AGENCY
WASHINGTON, DC 20301
ATTN DS-4A2

DIRECTOR
DEFENSE NUCLEAR AGENCY
WASHINGTON, DC 20305
ATTN DDST
ATTN RAEV
ATTN STTL TECH LIBRARY
ATTN STVL
ATTN RATN

ENERGY RESEARCH & DEVELOPMENT AGENCY
MATERIALS RADIATION EFFECTS BR
DIV OF CONTROLLED THERMONUCLEAR FUSION
WASHINGTON, DC 20545
ATTN MARVIN COHEN

COMMANDER
FIELD COMMAND
DEFENSE NUCLEAR AGENCY
KIRTLAND AFB, NM 87115
ATTN FCPR

DIRECTOR
INTERSERVICE NUCLEAR WEAPONS SCHOOL
KIRTLAND AFB, NM 87115
ATTN DOCUMENT CONTROL

DIRECTOR
JOINT STRATEGIC TARGET
PLANNING STAFF, JCS
OFFUTT AFB
OMAHA, NB 68113
ATTN JLTW-2

CHIEF
LIVERMORE DIVISION, FIELD COMMAND DNA
LAWRENCE LIVERMORE LABORATORY
P.O. BOX 808
LIVERMORE, CA 94550
ATTN DOCUMENT CONTROL FOR L-395
ATTN FCPRL

DIRECTOR
NATIONAL SECURITY AGENCY
FT. GEORGE G. MEADE, MD 20755
ATTN O. O. VAN GUNTEN-R-425
ATTN TDL

PROJECT MANAGER
ARMY TACTICAL DATA SYSTEMS
US ARMY ELECTRONICS COMMAND
FORT MONMOUTH, NJ 07703
ATTN DRCPN-TDS-SD
ATTN DWAINE B. HUEWE

COMMANDER
BMD SYSTEM COMMAND
PO BOX 1500
HUNTSVILLE, AL 35807
ATTN BDMSC, TEN, NOAH J. HURST

COMMANDER
FRANKFORD ARSENAL
BRIDGE AND TACONY STREETS
PHILADELPHIA, PA 19137
ATTN SARFA-FCD, MARVIN ELNICK

COMMANDER
PICATINNY ARSENAL
DOVER, NJ 07801
ATTN SARPA-ND-W
ATTN SARPA-TN, BURTON V. FRANKS
ATTN SARPA-ND-N
ATTN SARPA-ND-N-E
ATTN SARPA-FR-E, LOUIS AVRAMI

COMMANDER
REDSTONE SCIENTIFIC INFORMATION CTR
US ARMY MISSILE COMMAND
REDSTONE ARSENAL, AL 35809
ATTN CHIEF, DOCUMENTS

SECRETARY OF THE ARMY
WASHINGTON, DC 20310
ATTN ODUSA OR, DANIEL WILLIARD

COMMANDER
TRASANA
WHITE SANDS MISSILE RANGE, NM 88002
ATTN ATAA-EAC, FRANCIS N. WINANS

DIRECTOR
US ARMY BALLISTIC RESEARCH LABORATORIES
ABERDEEN PROVING GROUND, MD 21005
ATTN DRXBR-AM, W. R. VANANTWERP
ATTN DRXBD-BVL, DAVID L. RIGOTTI
ATTN DRXBR-X, JULIUS J. MESZAROS

COMMANDER
US ARMY COMMUNICATIONS SYSTEMS AGENCY
FORT MONMOUTH, NJ 07703
ATTN SCCM-AD-SV (LIBRARY)

COMMANDER
US ARMY ELECTRONICS COMMAND
FORT MONMOUTH, NJ 07703
ATTN DRSEL-CT-HDK, ABRAHAM E. COHEN
ATTN DRSEL-TL-MD, GERHART K. GAULE
ATTN DRSEL-TL-EN, ROBERT LUX
ATTN DRSEL-GG-TD, W. R. WERK
ATTN DRSEL-PL-ENV, HANS A. BOMKE
ATTN DRSEL-TL-ND, S. KRONENBEY
ATTN DRSEL-TL-IR, EDWIN T. HUNTER
ATTN DRSEL-TL-EN, E. BOTH

COMMANDER-IN-CHIEF
US ARMY EUROPE AND SEVENTH ARMY
APO NEW YORK 09403
ATTN ODCSE-E, AEAGE-PI

COMMANDER
US ARMY MISSILE COMMAND
REDSTONE ARSENAL, AL 35809
ATTN DRCPM-PE-EA, WALLACE O. WAGNER
ATTN DRSMI-RGD, VICTOR W. RUWE
ATTN DRSMI-RRR, FAISON P. GIBSON
ATTN DRCPM-MDTI, CPT JOE A SIMS
ATTN DRSMI-RGP, HUGH GREEN
ATTN DRCPM-LCEX, HOWARD H. HENRIKSEN

COMMANDER
US ARMY MOBILITY EQUIP R&D CTR
FORT BELVOIR, VA 22060
ATTN STSFB-MW, JOHN W. BOND, JR.

CHIEF
US ARMY NUC AND CHEMICAL SURETY GP
BLDG, 2073, NORTH AREA
FT. BELVOIR, VA 22060
ATTN MOSG-ND, MAJ SIDNEY W. WINSLOW

COMMANDER
US ARMY NUCLEAR AGENCY
FORT BLISS, TX 79916
ATTN ATCN-W, LTC LEONARD A. SLUGA

COMMANDER
US ARMY RESEARCH OFFICE
PO BOX 12211
RESEARCH TRIANGLE PARK, NC 27709
ATTN R. LONTZ

COMMANDER
US ARMY TEST AND EVALUATION COMMAND
ABERDEEN PROVING GROUND, MD 21005
ATTN DRSTE-EL, R. I. KOLCHIN
ATTN DRSTE-NB, R. R. GALASSO

CHIEF OF NAVAL RESEARCH
NAVY DEPARTMENT
ARLINGTON, VA 22217
ATTN CODE 421, DORAN W. PADGETT
ATTN CODE 427

COMMANDER
NAVAL ELECTRONIC SYSTEMS COMMAND
HEADQUARTERS
WASHINGTON, DC 20360
ATTN PME 117-21
ATTN ELEX 05323, CLEVELAND F. WATKINS
ATTN CODE 504510

COMMANDING OFFICER
NAVAL INTELLIGENCE SUPPORT CENTER
4301 SUITLAND ROAD, BLDG 5
WASHINGTON, DC 20390
ATTN P. ALEXANDER

DIRECTOR
NAVAL RESEARCH LABORATORY
WASHINGTON, DC 20375
ATTN CODE 6631, JAMES C. RITTER
ATTN CODE 4004, EMANUAL L. BRANCATO
ATTN CODE 2627, DORIS R. FOLEN
ATTN CODE 7701, JACK D. BROWN
ATTN CODE 5216, HAROLD L. HUGHES
ATTN CODE 5210, JOHN E. DAVEY
ATTN CODE 601, E. WOLICKI

COMMANDER
NAVAL SEA SYSTEMS COMMAND
NAVY DEPARTMENT
WASHINGTON, DC 20362
ATTN SEA-9931, RILEY B. LANE
ATTN SEA-9931, SAMUEL A. BARHAM

COMMANDER
NAVAL SHIP ENGINEERING CENTER
CENTER BUILDING
HYATTSVILLE, MD 20782
ATTN CODE 6174D2, EDWARD F. DUFFY

COMMANDER
NAVAL SURFACE WEAPONS CENTER
WHITE OAK, SILVER SPRING, MD 20910
ATTN CODE WA501, NAVY NUC PRGMS OFF
ATTN CODE WA50, JOHN H. MALLOY

COMMANDER
NAVAL SURFACE WEAPONS CENTER
DAHLGREN LABORATORY
DAHLGREN, VA 22448
ATTN WILLIAM H. HOLT

COMMANDER
NAVAL WEAPONS CENTER
CHINA LAKE, CA 93555
ATTN CODE 533, TECHNICAL LIBRARY

COMMANDING OFFICER
NAVAL WEAPONS SUPPORT CENTER
CRANE, IN 47522
ATTN CODE 70242, JOSEPH A. MUNARIN
ATTN CODE 7024, JAMES RAMSEY

COMMANDING OFFICER
NUCLEAR WEAPONS TRAINING CENTER PACIFIC
NAVAL AIR STATION, NORTH ISLAND
SAN DIEGO, CA 92135
ATTN CODE 50

DIRECTOR
STRATEGIC SYSTEMS PROJECT OFFICE
NAVY DEPARTMENT
WASHINGTON, DC 20376
ATTN NSP-2342, RICHARD L. COLEMAN

GEOPHYSICS LABORATORY
HANSCOM AFB, MA 01731
ATTN J. EMERY CORMIER
ATTN LQR, EDWARD A. BURKE

AF INSTITUTE OF TECHNOLOGY, AU
WRIGHT-PATTERSON AFB, OH 45433
ATTN ENP, CHARLES J. BRIDGMAN

AF MATERIALS LABOTATORY, AFSC
WRIGHT-PATTERSON AFB, OH 45433
ATTN LTE

AF WEAPONS LABORATORY, AFSC
KIRTLAND AFB, NM 87117
ATTN SAT
ATTN ELA
ATTN SAB

AFTAC
PATRICK AFB, FL 32925
ATTN TAE

HEADQUARTERS
ELECTRONIC SYSTEMS DIVISION, (AFSC)
L. G. HANSCOM FIELD
BEDFORD, MA 01730
ATTN YSEV, LTC DAVID C. SPARKS

COMMANDER
FOREIGN TECHNOLOGY DIVISION, AFSC
WRIGHT-PATTERSON AFB, OH 45433
ATTN ETET, CAPT RICHARD C. HUSEMANN

SAMSO/DY
POST OFFICE BOX 92960
WORLDWAY POSTAL CENTER
LOS ANGELES, CA 90009
ATTN DYS, CAPT WAYNE SCHOBER
ATTN DYS, MAJ LARRY A. DARDA

SAMSO/IN
POST OFFICE BOX 92960
WORLDWAY POSTAL CENTER
LOS ANGELES, CA 90009
ATTN IND, I. J. JUDY

SAMSO/MN
NORTON AFB, CA 92409
ATTN MNNG, CAPT DAVID J. STROBEL

SAMSO/RS
POST OFFICE BOX 92960
WORLDWAY POSTAL CENTER
LOS ANGELES, CA 90009
ATTN RSE
ATTN RSSE, LTC KENNETH L. GILBERT

SAMSO/SZ
POST OFFICE BOX 92960
WORLDWAY POSTAL CENTER
LOS ANGELES, CA 90009
ATTN SZJ, CAPT JOHN H. SAUCH

SAMSO/YD
POST OFFICE BOX 92960
WORLDWAY POSTAL CENTER
LOS ANGELES, CA 90009
ATTN YDD, MAJ M. F. SCHNEIDER

COMMANDER IN CHIEF
STRATEGIC AIR COMMAND
OFFUTT AFB, NB 68113
ATTN NRI-STINFO LIBRARY
ATTN XPFS, MAJ BRIAN STEPHAN

LOS ALAMOS SCIENTIFIC LABORATORY
P.O. BOX 1663
LOS ALAMOS, NM 87544
ATTN MARVIN M. HOFFMAN
ATTN J. ARTHUR FREED
ATTN BRUCE W. NOEL

SANDIA LABORATORIES
LIVERMORE LABORATORY
PO BOX 969
LIVERMORE, CA 94550
ATTN THEODORE A. DELLIN
ATTN P. L. MATTERN

SANDIA LABORATORIES
PO BOX 5800
ALBUQUERQUE, NM 87115
ATTN 3141 SANDIA RPT COLL
ATTN ORG 2110, J. A. HOOD
ATTN ORG 1933, F. N. COPPAGE
ATTN JACK V. WALKER, 5220
ATTN R. C. HUGHES
ATTN HOWARD SANDER
ATTN DIV 5231, JAMES H. RENKEN

US ENERGY RSCH & DEV ADMIN
ALBUQUERQUE OPERATIONS OFFICE
PO BOX 5400
ALBUQUERQUE, NM 87115
ATTN WSSB

UNIVERSITY OF CALIFORNIA
LAWRENCE LIVERMORE LABORATORY
PO BOX 808
LIVERMORE, CA 94550
ATTN DONALD J. MEEKER, L-545
ATTN HANS KRUGER, L-96
ATTN TECH INFO DEPT, L-3
ATTN LAWRENCE CLELAND, L-156
ATTN RONALD L. OTT, L-531
ATTN JOSEPH E. KELLER, JR., L-125
ATTN FREDERICK R. KOVAR, L-31

CENTRAL INTELLIGENCE AGENCY
ATTN RD/SI, RM 5G48, HQ BLDG
WASHINGTON, DC 20505
ATTN ALICE A. PADGETT

DEPARTMENT OF COMMERCE
NATIONAL BUREAU OF STANDARDS
WASHINGTON, DC 20234
ATTN JUDSON C. FRENCH
ATTN APPL RAD DIV
ROBERT C. PLACIOUS
ATTN SEMICONDUCTOR TECHNOLOGY,
W. M. BULLIS
ATTN K. F. GALLAWAY

AEROJET ELECTRO-SYSTEMS CO DIV
AEROJET-GENERAL CORPORATION
PO BOX 296
AZUSA, CA 91702
ATTN THOMAS D. HANSCOME

AERONUTRONIC FORD CORPORATION
AEROSPACE & COMMUNICATIONS OPS
AERONUTRONIC DIVISION
FORD & JAMBOREE ROADS
NEWPORT BEACH, CA 92663
ATTN KEN C. ATTINGER
ATTN TECH INFO SECTION

AERONUTRONIC FORD CORPORATION
WESTERN DEVELOPMENT LABORATORIES DIV
3939 FABIAN WAY
PALO ALTO, CA 94303
ATTN SAMUEL R. CRAWFORD, MS 531
ATTN DONALD R. MCMORROW, MS G30

AEROSPACE CORPORATION
PO BOX 92957
LOS ANGELES, CA 90009
ATTN IRVING M. GARFUNKEL
ATTN JULIAN REINHEIMER
ATTN LIBRARY
ATTN MELVIN J. BERNSTEIN
ATTN WILLIAM W. WILLIS
ATTN L. W. AUKERMAN

AVCO RESEARCH & SYSTEMS GROUP
201 LOWELL STREET
WILMINGTON, MA 01887
ATTN RESEARCH LIBRARY, A830, RM 7201

BDM CORPORATION, THE
PO BOX 9274
ALBUQUERQUE INTERNATIONAL
ALBUQUERQUE, NM 87119
ATTN T. H. NEIGHBORS

BENDIX CORPORATION, THE
COMMUNICATION DIVISION
EAST JOPPA ROAD - TOWSON
BALTIMORE, MD 21204
ATTN DOCUMENT CONTROL

BENDIX CORPORATION, THE
RESEARCH LABORATORIES DIV
BENDIX CENTER
SOUTHFIELD, MI 48075
ATTN MGR PRGM DEV,
DONALD J. NIEHAUS

BOEING COMPANY, THE
PO BOX 3707
SEATTLE, WA 98124
ATTN HOWARD W. WICKLEIN, MS 17-11
ATTN DAVID DYE, MS 87-75
ATTN AEROSPACE LIBRARY
ATTN ROBERT S. CALDWELL, 2R-00

BOOZ-ALLEN AND HAMILTON, INC.
106 APPLE STREET
NEW SHREWSBURY, NJ 07724
ATTN R. J. CHRISNER

CALIFORNIA INSTITUTE OF TECHNOLOGY
JET PROPULSION LABORATORY
4800 OAK GROVE
PASADENA, CA 91103
ATTN A. G. STANLEY
ATTN J. BRYDEN

CHARLES STARK DRAPER LABORATORY INC.
68 ALBANY STREET
CAMBRIDGE, MA 02139
ATTN KENNETH FERTIG
ATTN RICHARD G. HALTMAIER
ATTN PAUL R. KELLY

COMPUTER SCIENCES CORPORATION
201 LA VETA DRIVE, NE
ALBUQUERQUE, NM 87108
ATTN RICHARD H. DICKHAUT

C. T. SAH ASSOCIATES
PO BOX 364
URBANA, IL 61801
ATTN C. T. SAH

CUTLER-HAMMER, INC.
AIL DIVISION
COMAC ROAD
DEER PARK, NY 11729
ATTN CENTRAL TECH FILES,
ANN ANTHONY

DIKEWOOD CORPORATION, THE
1009 BRADBURY DRIVE, SE
UNIVERSITY RESEARCH PARK
ALBUQUERQUE, NM 87106
ATTN L. WAYNE DAVIS

E-SYSTEMS, INC.
GREENVILLE DIVISION
PO BOX 1056
GREENVILLE, TX 75401
ATTN LIBRARY 8-50100

EFFECTS TECHNOLOGY, INC.
5383 HOLISTER AVENUE
SANTA BARBARA, CA 93105
ATTN EDWARD JOHN STEELE

ELECTRONICS TECHNOLOGY LABORATORY
ENGINEERING EXPERIMENT STATION
GEORGIA INSTITUTE OF TECHNOLOGY
ATLANTA, GA 30332
ATTN R. CURRY

EXPERIMENTAL AND MATHEMATICAL
PHYSICS CONSULTANTS
P. O. BOX 66331
LOS ANGELES, CA 90066
ATTN THOMAS M. JORDAN

FAIRCHILD CAMERA AND
INSTRUMENT CORPORATION
464 ELLIS STREET
MOUNTAIN VIEW, CA 94040
ATTN 2-233, MR. DAVID K. MYERS

FAIRCHILD INDUSTRIES, INC.
SHERMAN FAIRCHILD TECHNOLOGY CENTER
20301 CENTURY BOULEVARD
GERMANTOWN, MD 20767
ATTN MGR CONFIG DATA & STANDARDS

UNIVERSITY OF FLORIDA
231 AEROSPACE BLDG
GAINSVILLE, FL 32611
ATTN D. P. KENNEDY

FRANKLIN INSTITUTE, THE
20TH STREET AND PARKWAY
PHILADELPHIA, PA 19103
ATTN RAMIE H. THOMPSON

GENERAL DYNAMICS CORP
ELECTRONICS DIV ORLANDO OPERATIONS
PO BOX 2566
ORLANDO, FL 32802
ATTN D. W. COLEMAN

GENERAL ELECTRIC COMPANY
SPACE DIVISION
VALLEY FORGE SPACE CENTER
P.O. BOX 8555
PHILADELPHIA, PA 19101
ATTN JAMES P. SPRATT
ATTN LARRY I. CHASEN
ATTN JOSEPH C. PEDEN, CCF 8301
ATTN JOHN L. ANDREWS

GENERAL ELECTRIC COMPANY
RE-ENTRY & ENVIRONMENTAL SYSTEMS DIV
PO BOX 7722
3198 CHESTNUT STREET
PHILADELPHIA, PA 19101
ATTN ROBERT V. BENEDICT

GENERAL ELECTRIC COMPANY
ORDNANCE SYSTEMS
100 PLASTICS AVENUE
PITTSFIELD, MA 01201
ATTN JOSEPH J. REIDL

GENERAL ELECTRIC COMPANY
TEMPO-CENTER FOR ADVANCED STUDIES
816 STATE STREET (PO DRAWER QQ)
SANTA BARBARA, CA 93102
ATTN DASIAC
ATTN ROYDEN R. RUTHERFORD
ATTN M ESPIG

GENERAL ELECTRIC COMPANY
PO BOX 1122
SYRACUSE, NY 13201
ATTN CSP 6-7, RICHARD C. FRIES
ATTN CSP 0-7, L. H. DEE

GENERAL ELECTRIC COMPANY
AIRCRAFT ENGINE GROUP
EVENDALE PLANT
CINCINNATI, OH 45215
ATTN JOHN A. ELLERHORST, E2

GENERAL ELECTRIC COMPANY
AEROSPACE ELECTRONICS SYSTEMS
FRENCH ROAD
UTICA, NY 13503
ATTN W. J. PATTERSON, DROP 233

GENERAL ELECTRIC COMPANY
PO BOX 5000
BINGHAMTON, NY 13902
ATTN DIVID W. PEPIN, DROP 160

GENERAL ELECTRIC COMPANY-TEMPO
ATTN: DASIAC
C/O DEFENSE NUCLEAR AGENCY
WASHINGTON, DC 20305
ATTN WILLIAM ALFONTE

DISTRIBUTION (Cont'd)

GENERAL RESEARCH CORPORATION
P.O. BOX 3587
SANTA BARBARA, CA 93105
ATTN ROBERT D. HILL

GRUMMAN AEROSPACE CORPORATION
SOUTH OYSTER BAY ROAD
BETHPAGE, NY 11714
ATTN JERRY ROGERS, DEPT 532

GTE SYLVANIA, INC.
ELECTRONICS SYSTEMS GRP-EASTERN DIV
77 A STREET
NEEDHAM, MA 02194
ATTN CHARLES A. THORNHILL, LIBRARIAN
ATTN LEONARD L. BLAISDELL
ATTN JAMES A. WALDON

GTE SYLVANIA, INC.
189 B STREET
NEEDHAM HEIGHTS, MA 02194
ATTN CHARLES H. RAMSBOTTOM
ATTN HERBERT A. ULLMAN
ATTN H & V GROUP, MARIO A. NUREFORA
ATTN PAUL B. FREDRICKSON

HARRIS CORPORATION
HARRIS SEMICONDUCTOR DIVISION
P.O. BOX 883
MELBOURNE, FL 32901
ATTN C. F. DAVIS, MS 17-220
ATTN T. CLARK, MS 4040
ATTN WAYNE E. ABARE, MS 16-111

HAZELTINE CORPORATION
PULASKI ROAD
GREEN LAWN, NY 11740
ATTN TECH INFO CTR, M. WAITE

HONEYWELL INCORPORATED
GOVERNMENT AND AERONAUTICAL
PRODUCTS DIVISION
2600 RIDGEWAY PARKWAY
MINNEAPOLIS, MN 55413
ATTN RONALD R. JOHNSON, A1622

HONEYWELL INCORPORATED
AEROSPACE DIVISION
13350 US HIGHWAY 19
ST. PETERSBURG, FL 33733
ATTN MS 725-J, STACEY H. GRAFF

HONEYWELL INCORPORATED
RADIATION CENTER
2 FORBES ROAD
LEXINGTON, MA 02173
ATTN TECHNICAL LIBRARY

HUGHES AIRCRAFT COMPANY
CENTINELA & TEALE
CULVER CITY, CA 90230
ATTN M.S. D157, KEN WALKER
ATTN B. W. CAMPBELL, M.S. 6-E110
ATTN DAN BINDER, MS 6-D147

HUGHES AIRCRAFT COMPANY
SPACE SYSTEMS DIVISION
P.O. BOX 92919
LOS ANGELES, CA 90009
ATTN WILLIAM W. SCOTT, MS A1080
ATTN EDWARD C. SMITH, MS A620

HUGHES AIRCRAFT COMPANY
500 SUPERIOR AVE
NEWPORT BEACH, CA 92663
ATTN KENNETH AUBUCHON
ATTN ELI HARARI

IBM CORPORATION
ROUTE 17C
OWEGO, NY 13827
ATTN FRANK FRANKOVSKY

INTELCOM RAD TECH
P.O. BOX 81087
SAN DIEGO, CA 92138
ATTN ROLAND LEADON
ATTN T. M. FLANAGAN

ION PHYSICS CORPORATION
SOUTH BEDFORD STREET
BURLINGTON, MA 01803
ATTN ROBERT D. EVANS

IRT CORPORATION
PO BOX 81087
SAN DIEGO, CA 92138
ATTN MDC
ATTN JAMES A. NABER
ATTN RALPH H. STAHL
ATTN R. L. MERTZ

KAMAN SCIENCES CORPORATION
P.O. BOX 7463
COLORADO SPRINGS, CO 80933
ATTN DONALD H. BRYCE
ATTN ALBERT P. BRIDGES
ATTN WALTER E. WARE

LEHIGH UNIVERSITY
MATERIALS RESEARCH CENTER
BETHLEHEM, PA 18015
ATTN S. R. BUTLER
ATTN F. J. FEIGL
ATTN F. M. FOWKES

LITTON SYSTEMS, INC.
GUIDANCE & CONTROL SYSTEMS DIVISION
5500 CANOGA AVENUE
WOODLAND HILLS, CA 91364
ATTN VAL J. ASHBY, MS 67
ATTN JOHN P. RETZLER

LOCKHEED MISSILES AND SPACE
COMPANY, INC.
P.O. BOX 504
SUNNYVALE, CA 94088
ATTN G. F. HEATH, D/81-14
ATTN BENJAMIN T. KIMURA,
DEPT 81-14, BLDG 154
ATTN EDWIN A. SMITH, DEPT 85-85
ATTN PHILIP J. HART, DEPT 81-14
ATTN L. ROSSI, DEPT 81-64
ATTN DEPT 81-01, G. H. MORRIS

LOCKHEED MISSILES AND SPACE COMPANY
3251 HANOVER STREET
PALO ALTO, CA 94304
ATTN TECH INFO CTR D/COLL

LTV AEROSPACE CORPORATION
VOUGHT SYSTEMS DIVISION
P.O. BOX 6267
DALLAS, TX 75222
ATTN TECHNICAL DATA CENTER

LTV AEROSPACE CORPORATION
PO BOX 5907
DALLAS, TX 75222
ATTN TECHNICAL DATA CTR

M.I.T. LINCOLN LABORATORY
P.O. BOX 73
LEXINGTON, MA 02173
ATTN LEONA LOUGHLIN, LIBRARIAN A-082

MARTIN MARIETTA AEROSPACE
ORLANDO DIVISION
P.O. BOX 5837
ORLANDO, FL 32805
ATTN MONA C. GRIFFITH, LIB MP-30
ATTN WILLIAM W. MRAS, MP-413

MARTIN MARIETTA CORPORATION
DENVER DIVISION
PO BOX 179
DENVER, CO 80201
ATTN J. E. GOODWIN, MAIL 0452
ATTN RESEARCH LIB, 6617, J. R. MCKEE
ATTN BEN T. GRAHAM, MS PO-454

MCDONNELL DOUGLAS CORPORATION
POST OFFICE BOX 516
ST. LOUIS, MO 63166
ATTN TECHNICAL LIBRARY

MCDONNELL DOUGLAS CORPORATION
5301 BOLSA AVENUE
HUNTINGTON BEACH, CA 92647
ATTN STANLEY SCHNEIDER

MISSION RESEARCH CORPORATION
735 STATE STREET
SANTA BARBARA, CA 93101
ATTN WILLIAM C. HART

MISSION RESEARCH CORPORATION-SAN DIEGO
7650 CONVOY COURT
SAN DIEGO, CA 92111
ATTN V. A. J. VAN LINT

NATIONAL ACADEMY OF SCIENCES
2101 CONSTITUTION AVE, NW
WASHINGTON, DC 20418
ATTN DR. R. S. SHANE,
NAT MATERIALS ADVISORY BOARD

UNIVERSITY OF NEW MEXICO
DEPT OF CAMPUS SECURITY AND POLICE
1821 ROMA NE
ALBUQUERQUE, NM 87106
ATTN W. W. GRANNEMANN

NORTHROP CORPORATION
ELECTRONIC DIVISION
1 RESEARCH PARK
PALOS VERDES PENINSULA, CA 90274
ATTN VINCENT R. DEMARTINO
ATTN BOYCE T. AHLPORT
ATTN GEORGE H. TOWNER

NORTHROP CORPORATION
NORTHROP RESEARCH AND TECHNOLOGY CENTER
3401 WEST BROADWAY
HAWTHORNE, CA 90250
ATTN DAVID N. POCOCK
ATTN JOSEPH R. SROUR

PHYSICS INTERNATIONAL COMPANY
2700 MERCED STREET
SAN LEANDRO, CA 94577
ATTN CHARLES H. STALLINGS
ATTN JOHN H. HUNTINGTON

PRINCETON UNIVERSITY
DEPT OF AEROSPACE &
MECHANICAL SCIENCES
PRINCETON, NJ 08940
ATTN BARRIE S. H. ROYCE

R & D ASSOCIATES
PO BOX 9695
MARINA DEL REY, CA 90291
ATTN S. CLAY ROGERS

RAYTHEON COMPANY
HARTWELL ROAD
BEDFORD, MA 01730
ATTN GAJANAN H. JOSHI,
RADAR SYS LAB

RCA CORPORATION
GOVERNMENT & COMMERCIAL SYSTEMS
ASTRO ELECTRONICS DIVISION
PO BOX 800, LOCUST CORNER
PRINCETON, NJ 08540
ATTN GEORGE J. BRUCKER

RCA CORPORATION
DAVID SARNOFF RESEARCH CENTER
W. WINDSOR TWP
201 WASHINGTON ROAD, PO BOX 432
PRINCETON, NJ 08540
ATTN K. H. ZAININGER
ATTN R. J. POWELL

RENSSELAER POLYTECHNIC INSTITUTE
PO BOX 965
TROY, NY 12181
ATTN RONALD J. GUTMANN

RESEARCH TRIANGLE INSTITUTE
PO BOX 12194
RESEARCH TRIANGLE PARK, NC 27709
ATTN ENG DIV, MAYRANT SIMONS, JR.

ROCKWELL INTERNATIONAL CORPORATION
3370 MIRALOMA AVENUE
ANAHEIM, CA 92803
ATTN K. F. HULL
ATTN JAMES E. BELL, HA10
ATTN DONALD J. STEVENS, FA70
ATTN GEORGE C. MESSENGER, FB61

ROCKWELL INTERNATIONAL CORPORATION
ELECTRONICS OPERATIONS
COLLINS RADIO GROUP
5225 C. AVE NE
CEDAR RAPIDS, IA 52406
ATTN DENNIS SUTHERLAND

SANDERS ASSOCIATES, INC.
95 CANAL STREET
NASHUA, NH 03060
ATTN M. L. AITEL, NCA 1-3236

SCIENCE APPLICATIONS, INC.
1651 OLD MEADOW ROAD
MCLEAN, VA 22101
ATTN WILLIAM L. CHADSEY

SCIENCE APPLICATIONS, INC.
PO BOX 2351
LA JOLLA, CA 92038
ATTN LARRY SCOTT
ATTN J. ROBERT BEYSTER

SCIENCE APPLICATIONS, INC.
HUNTSVILLE DIVISION
2109 W. CLINTON AVENUE
SUITE 700
HUNTSVILLE, AL 35805
ATTN NOEL R. BYRN

SCIENCE APPLICATIONS, INC.
2680 HANOVER STREET
PALO ALTO, CA 94303
ATTN CHARLES STEVENS

SIMULATION PHYSICS, INC.
41 "B" STREET
BURLINGTON, MA 01803
ATTN ROGER G. LITTLE

SINGER COMPANY, THE
1150 MC BRIDE AVENUE
LITTLE FALLS, NJ 07424
ATTN IRWIN GOLDMAN, ENG MANAGEMENT

SINGER COMPANY (DATA SYSTEMS), THE
150 TOTOWA ROAD
WAYNE, NJ 07470
ATTN TECH INFO CENTER

SPERRY RAND CORPORATION
SPERRY DIVISION
SPERRY GYROSCOPE DIVISION
SPERRY MANAGEMENT DIVISION
MARCUS AVENUE
GREAT NECK, NY 11020
ATTN PAUL MARRAFFINO
ATTN CHARLES L. CRAIG EV

STANFORD RESEARCH INSTITUTE
333 RAVENSWOOD AVENUE
MENLOW PARK, CA 94025
ATTN MR. PHILIP DOLAN
ATTN ROBERT A. ARMISTEAD

STANFORD RESEARCH INSTITUTE
306 WYNN DRIVE, N. W.
HUNTSVILLE, AL 35805
ATTN MACPHERSON MORGAN

SUNDSTRAND CORPORATION
4751 HARRISON AVENUE
ROCKFORD, IL 61101
ATTN DEPT 763SW, CURTIS WHITE

TEXAS INSTRUMENTS, INC.
P.O. BOX 5474
DALLAS, TX 75222
ATTN DONALD J. MANUS, MS 72

TRW SYSTEMS GROUP
ONE SPACE PARK
REDONDO BEACH, CA 90278
ATTN R. D. LOVELAND, R1-1028
ATTN A. A. WITTELES, MS R1-1120
ATTN TECH INFO CENTER/S-1930
ATTN A. M. LIEBSCHUTZ R1-1162
ATTN AARON H. NAREVSKY, R1-2144
ATTN RICHARD H. KINGSLAND, R1-2154
ATTN JERRY I. LUBELL
ATTN LILLIAN D. SINGLETARY, R1/1070
ATTN WILLIAM H. ROBINETTE, JR.
ATTN PAUL MOLMUD, R1-1196
ATTN ALLAN ANDERMAN, R1-1132

TRW SYSTEMS GROUP
SAN BERNARDINO OPERATIONS
PO BOX 1310
SAN BERNARDINO, CA 92402
ATTN EARL W. ALLEN
ATTN JOHN E. DAHNKE
ATTN H. S. JENSEN

WESTINGHOUSE ELECTRIC CORPORATION
DEFENSE AND ELECTRONIC SYSTEMS CENTER
P.O. BOX 1693
FRIENDSHIP INTERNATIONAL AIRPORT
BALTIMORE, MD 21203
ATTN HENRY P. KALAPACA, MS 3525

WESTINGHOUSE ELECTRIC CORPORATION
RESEARCH AND DEVELOPMENT CENTER
1310 BEULAH ROAD, CHURCHILL BOROUGH
PITTSBURGH, PA 15235
ATTN WILLIAM E. NEWELL

COMMANDER
HARRY DIAMOND LABORATORIES
2800 POWDER MILL RD
ADELPHI, MD 20783
ATTN MCGREGOR, THOMAS, COL, COMMANDING
OFFICER/FLYER, I.N./LANDIS, P.E./
SOMMER, H./CONRAD, E.E.
ATTN CARTER, W.W., DR., ACTING TECHNICAL
DIRECTOR/MARCUS, S.M.
ATTN KIMMEL, S., IO
ATTN CHIEF, 0021
ATTN CHIEF, 0022
ATTN CHIEF, LAB 100
ATTN CHIEF, LAB 200
ATTN CHIEF, LAB 300
ATTN CHIEF, LAB 400
ATTN CHIEF, LAB 500
ATTN CHIEF, LAB 600
ATTN CHIEF, DIV 700
ATTN CHIEF, DIV 800
ATTN CHIEF, LAB 900
ATTN CHIEF, LAB 1000
ATTN RECORD COPY, BR 041
ATTN HDL LIBRARY (3 COPIES)
ATTN CHAIRMAN, EDITORIAL COMMITTEE
ATTN CHIEF, 047
ATTN TECH REPORTS, 013
ATTN PATENT LAW BRANCH, 071
ATTN MCLAUGHLIN, P.W., 741
ATTN THOMPKINS, J. E., LAB 200
ATTN CHIEF, BR 230
ATTN ROSADO, J. A., 240
ATTN CHIEF, BR 280
ATTN CALDWELL, P. A., 290
ATTN SCHALLHORN, D. R., 230
ATTN OLDHAM, T. R., 230
ATTN SCHARF, W. D., 230
ATTN BOESCH, H. E., JR. 280
ATTN WINOKUR, P. S., 280
ATTN WINEMITZ, F. N., 0024
ATTN MCGARRITY, J. M., 280
ATTN SOKOLOSKI, M. M., 0021
ATTN AUSMAN, G. A., 210
ATTN MCLEAN, F. B. (20 COPIES)